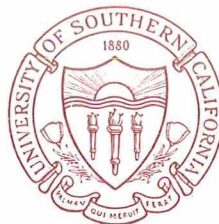


N 70 42094
CR 114115

USCEE Report 396

August 1970



UNIVERSITY OF SOUTHERN CALIFORNIA

Optical Synchronization-Phase Locking
With Shot Noise Processes

R. Gagliardi

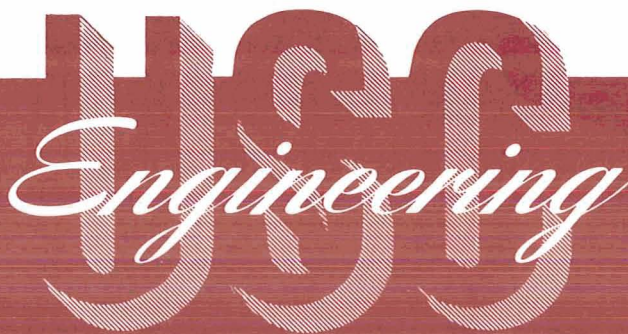
M. Haney

Interim Technical Report

Department of Electrical Engineering
University of Southern California
Los Angeles, California 90007

This work was sponsored by the National Aeronautics and Space Administration, under NASA Contract NGR-05-018-104. This grant is part of the research program initiated at NASA's Electronics Research Center, Cambridge, Massachusetts and continued at Goddard Space Flight Center, Greenbelt, Maryland.

ELECTRONIC SCIENCES LABORATORY



CASE FILE
COPY

August, 1970

Optical Synchronization-Phase Locking
With Shot Noise Processes

R. Gagliardi
M. Haney

Interim Technical Report

Department of Electrical Engineering
University of Southern California
Los Angeles, California 90007

This work was sponsored by the National Aeronautics and Space Administration, under NASA Contract NGR-05-018-104. This grant is part of the research program initiated at NASA's Electronics Research Center, Cambridge, Massachusetts and continued at Goddard Space Flight Center, Greenbelt, Maryland.

This document represents a technical report of a NASA Research Program to study synchronization techniques for optical communication systems. The work is being carried out at the Electrical Engineering Department at the University of Southern California, under NASA Contract No. NGR-05-018-104, with Professor R.M. Gagliardi as principal investigator. This grant is part of the research program being conducted through NASA's Goddard Space Flight Center, Greenbelt, Maryland.

Abstract

This report presents the results of a study effort examining time synchronization in an optical communication system. Consideration is given primarily to time locking by means of a phase lock tracking loop. Since photo-detection of an intensity modulated optical beam produces a shot noise random process at its output, synchronization analysis requires a study of phase locking with shot noise processes. A statistical analysis of tracking shot noise is presented. Of particular interest is the probability density of the tracking error, which indicates the behavior of the loop during tracking, and therefore is directly related to the ability to maintain accurate synchronization. The results of the study also have application to ranging and doppler tracking using optical systems.

Table of Contents

	Page
Abstract	i
Chapter	
1. Introduction	1
1.1 The Photo-Detection Model	2
1.2 Delay Locked and Phase Locked Loops	5
2. Error Equations For Phase Lock Loops	9
2.1 Derivation of Loop Error Dynamics	9
2.2 Probability Density Equations of Random Processes	14
2.3 Probability Density Equations of Tracking Errors	18
3. Probability Density Solutions	27
3.1 High Electron Density Solution	27
3.2 Higher Order Approximations	30
3.3 Second Order Approximations	34
3.4 Third Order Approximations	40
3.5 Accuracy of Truncation Solutions	43
3.6 The VCO Offset Case	46
4. Thermal Noise and Photomultiplier Effects	50
4.1 Additive Gaussian Thermal Noise	50
4.2 Effect of Photomultiplication	53
5. Second Order Loop Analyses and General Tracking Loops	57
5.1 The Two Dimensional Smoluchowski Equation	57
5.2 Second Order Phase Lock Loops	58
5.3 General Delay Tracking Loops	62
5.4 Example--Early-Late Gate Tracking	64
References	68

Chapter 1

INTRODUCTION

An important operation in communication systems is the maintenance of synchronization between transmitter and receiver. This is generally accomplished by transmitting continuously over a separate channel a known periodic waveform, and having a subsystem of the receiver continually track the waveform, thereby providing timing information for the entire receiver operation. The tracking is most typically accomplished by a delay locked loop which tracks the instantaneous time delay of the received synchronizing signal.

In an optical communication system, the synchronizing signal is often transmitted as an intensity modulated optical (laser) beam, which is photo-detected at the receiver. The subsequent timing operation is then achieved by time locking the receiver delay locked loop to the photo-detector output. Since photo-detection of an intensity modulated optical beam produces a shot noise random process at its output, the analysis of the synchronization subsystem requires careful study of the problem of time locking with shot noise input functions. In this report we present results of a study of the statistical analysis of tracking shot noise processes. Of particular interest is the probability density of the tracking error, which indicates the behavior of the loop during the tracking operation, and therefore is directly related to the ability to maintain accurate synchronization. The results of the study also have application to ranging and doppler tracking using optical systems.

1.1 The Photo-Detection Model

The overall block diagram of the sync subsystem is shown in Figure 1. The optical beam is intensity (power) modulated with a synchronizing signal. A point source photo-detection responds to the received optical radiation by producing the output shot noise process [6, 7]

$$x(t) = \sum_{m=1}^{N(0,t)} e h(t-t_m) \quad (1-1)$$

where e is the electron charge, $h(t)$ is the photo-electron waveshape in the photo-detector, t_m are the random location times of each photo-electron and $N(0, t)$ is the number of photo-electrons occurring during the time interval $(0, t)$. The random process $N(0, t)$ is called the counting process of the shot noise and has a mean value given by [2, 3, 4]

$$\bar{N} = \int_0^t n(y) dy \quad (1-2)$$

where

$n(t) = \gamma P(t) =$ intensity of the counting process, or average rate of photo-electron occurrences.

$P(t) =$ instantaneous power in the received optical field.

$\gamma =$ proportionality constant dependent upon the optical carrier frequency, Planck's constant, and the detector efficiency.

Note that the average rate of photo-electron occurrences is proportional to $P(t)$, the power modulation on the optical beam. This means that in the case of optical synchronization, the intensity process $n(t)$ in (1-2) is directly proportional to the synchronizing signal that power modulates the optical beam.

When the bandwidth of the photo-detector is large relative to the bandwidth of the intensity $n(t)$, the electron functions in (1-1) can be

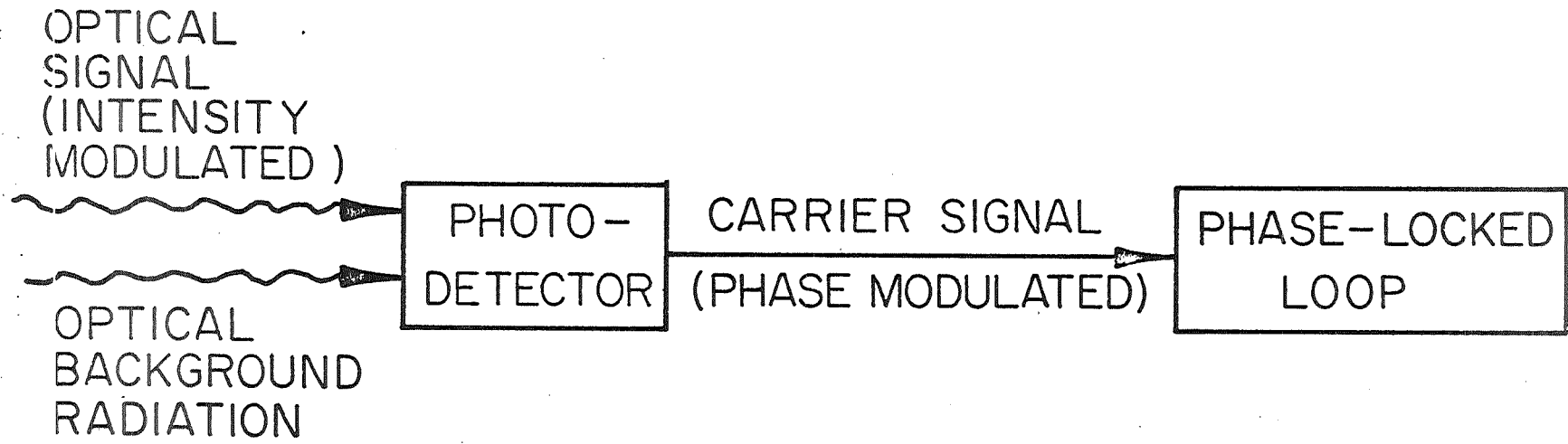


Figure 1.

considered as delta functions. In addition, $N(0, t)$ becomes a Poisson counting process [5, 6, 8], and the probability of j photo-electrons occurring in an interval $(0, t)$ is given by

$$\text{Prob}[N(0, t) = j] = \frac{\bar{N}^j}{j!} e^{-\bar{N}} \quad (1-3)$$

For shot noise process governed by Poisson counting, the random location times are independent, and have the probability density [5, 9, 10]

$$P(t_m) = \frac{n(t_m)}{\bar{N}} \quad (1-4)$$

where \bar{N} is the average of $N(0, t)$ in (1-3) and is given in (1-2). Thus, the intensity process $n(t)$, in addition to specifying the average rate of electron occurrences, also defines the probability density of location times of the electrons. Using (1-3) and (1-4) it can be shown [5, 6] that the mean of the shot noise $x(t)$ in (1-1) is

$$[\text{mean } x(t)] = \int_0^t \delta(t-y) n(y) dy = n(t) \quad (1-5)$$

for wideband detectors. Hence, the mean of the photo-detector output in Figure 1 corresponds to the synchronizing signal used at the transmitter.

1.2 Delay Locked and Phase Locked Loops

A delay locked loop is a feedback tracking system used to time lock a locally generated periodic signal to the received periodic synchronizing signal. During each period, the two signals are time compared, and differences in timing generate error voltages that are fed back to control the timing of the local signal generator. The choice of signals at the transmitter and receiver determine the sensitivity of the error voltage to the timing difference. When the two signals are exactly in step during each period, the error voltage is zero, and the local signal remains time synchronized with the received sync signal. When this occurs, the local signal generator is producing a clean, time locked signal that can be used for timing in the remainder of the receiver. Instantaneous error voltages due to input noise represent random timing errors between the two signals, and therefore appear as synchronization errors in the receiver operation.

When the synchronizing and local signal are taken as sinusoids, the delay locked loop is called a phase lock loop [1] (since timing errors can be directly related to phase errors in the sinusoids). In phase lock loops, the signal generator is simply a voltage controlled oscillator (VCO), and the timing difference is produced in a filtered frequency mixer, as shown in Figure 2. The phase variation on the synchronizing sinusoid is then the phase signal that is to be tracked by the loop.

For example, if the synchronizing signal were taken as $\sin[\omega_j t + \theta_1(t)]$, then the loop must generate an error voltage that drives the local VCO in accordance with $\theta_1(t)$.

The loop filter in Figure 2 smooths the error voltage for control of the VCO. The complexity of the loop, and of the associated analysis,

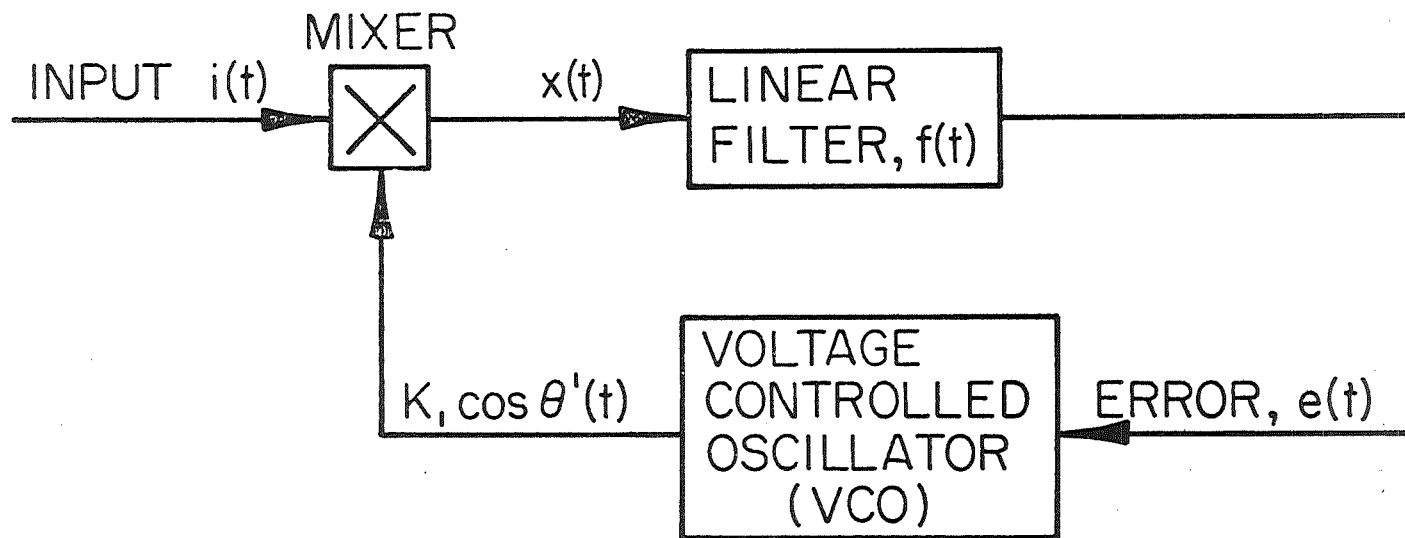


Figure 2.

is determined by the type of filtering used. For a first order loop, the filter is removed and the mixer error signal feeds directly the VCO. A second order loop is produced if the loop filter effectively produces an integration. Higher order loops are generated by introducing more filter integration.

The loop mixer simply "beats" together the input and VCO sinusoid. Since the mixer is inherently bandlimited, only baseband frequencies are produced at the mixer output, while harmonics of the VCO center frequency are eliminated.

The error voltage in a phase lock loop is directly related to the phase difference between the VCO and the loop input signal at each instant of time. Hence, analytical measures of loop performance can be obtained through derivation of the loop error equations. Though these equations are generally nonlinear, the response of the loop to a "clean" synchronizing signal can usually be determined using basic nonlinear feedback analysis. Typically, the loop "pulls into" lock and the steady state loop error is driven to zero, or else the system is unstable and the loop "falls out" of lock. On the other hand, when the loop input is stochastic, the loop error responds in a random manner. In this case one can only describe the error statistically by its probability density. The derivation of this density, which is generally non-stationary, is complicated by the non-linearity of the loop. Often, we resort to a steady state density as an indication of the statistical loop behavior. The steady state variance of the loop error is then a direct indication of the phase error caused by the randomness of the input.

In the past [1, 11] the above analytical procedures have been extensively applied to the case where the input randomness is due to

additive Gaussian noise; i. e., the loop input is composed of the sum of a clean synchronizing signal plus additive Gaussian noise. However, in the optical model of Figure 1, the randomness at the loop input is due to the shot noise nature of the photo-detector output. The remainder of this report is devoted to an investigation of the loop phase error when the phase lock loop in Figure 2 is forced by the input shot noise process in (1-1).

Chapter 2

ERROR EQUATIONS FOR PHASE LOCK LOOPS

In this chapter we analytically investigate the ability of a phase lock loop to lock to a synchronizing signal that has been optically transmitted and photo-detected. Mathematically, the basic problem is that of determining the behavior of a phase lock loop when its input is a shot noise process having the synchronizing signal as its intensity process. In the following section, we derive the dynamical equations that describe the evolution of the phase error for such a system.

2.1 Derivation of Loop Error Dynamics

Consider the system shown in Figure 2 where the loop input function is the shot noise process at the wideband photo-detector output, given by (1-1):

$$x(t) = \sum_{m=1}^{N(0,t)} e \delta(t-t_m) \quad . \quad (2-1)$$

Here, e is the electron charge, $\{t_m\}$ are the random location times, $\delta(t)$ the electron functions and $N(0,t)$ is the shot noise counting process having intensity

$$n_s(t) = A \{ 1 + b \sin[\omega_s t + \theta_1(t)] \} \quad (2-2)$$

The above is proportional to the transmitted intensity modulation and represents the synchronizing signal. In (2-2), ω_s is the synchronizing frequency, b is the modulation index, $\theta_1(t)$ is the phase (time delay) variation on the synchronizing signal that is to be instantaneously tracked by the loop and A is the average value of $n_s(t)$. Recall from (1-2) that $n_s(t)$ can equivalently be interpreted as the rate of electron occurrences

in the photo-detector, so that A represents the average number of electrons produced per sec.

The VCO output in Figure 2 is represented by

$$\text{VCO output} = k_1 \cos[\omega_0 t + \theta_2(t)] \quad (2-3)$$

where k_1 is the VCO gain, ω_0 is the VCO rest frequency, and $\theta_2(t)$ its phase variation. The loop phase error is defined as the phase difference between the synchronizing signal phase and the loop VCO phase, and therefore is

$$\Phi(t) \equiv [\omega_s t + \theta_1(t)] - [\omega_0 t + \theta_2(t)] = (\omega_s - \omega_0)t + \theta_1(t) - \theta_2(t) . \quad (2-4)$$

The loop mixer output is then

$$\begin{aligned} e_m(t) &= x(t) [\text{VCO output}] \\ &= k_1 \cos[\omega_0 t + \theta_2(t)] \left[\sum_{m=1}^{N(0,t)} e^{\delta(t-t_m)} \right] \end{aligned} \quad (2-5)$$

and the loop filter output is

$$e_f(t) = \int_0^t e_m(\tau) f(t-\tau) d\tau . \quad (2-6)$$

The VCO output phase responds to the VCO input control voltage $e_f(t)$ through the linear relation

$$\frac{d\theta_2(t)}{dt} = k_2 e_f(t) \quad (2-7)$$

with k_2 a constant of proportionality. From (2-4) we have, upon differentiating,

$$\begin{aligned} \frac{d\Phi(t)}{dt} &= (\omega_s - \omega_0) + \frac{d\theta_1}{dt} - \frac{d\theta_2}{dt} \\ &= (\omega_s - \omega_0) + \frac{d\theta_1}{dt} - k_2 e_f(t). \end{aligned} \quad (2-8)$$

The term $(\omega_s - \omega_0)$ is the difference between the input synchronizing frequency and the VCO rest frequency and is called the frequency "offset" of the loop. Substitution from (2-6) then yields

$$\begin{aligned} \frac{d\Phi}{dt} &= (\omega_s - \omega_0) + \frac{d\theta_1}{dt} - e k \int_0^t f(t-\tau) \cos[\omega_s \tau + \theta_1(\tau) - \Phi(\tau)] \cdot \\ &\quad \sum_{m=1}^{N(0, \tau)} \delta(\tau - t_m) d\tau \end{aligned} \quad (2-9)$$

where $k = k_1 k_2$, and can be interpreted as the total gain around the loop. Equation (2-9) is then the stochastic integro-differential equation that describes the behavior of the loop phase error in terms of the input signal and loop parameters. Note that it is a non-linear equation with $\Phi(t)$ appearing on both sides of the equation. The input shot noise and the phase variation of the transmitted synchronizing signal play the role of "forcing" functions in the generation of the error process. Since the input shot noise contains random parameters, the solution for $\Phi(t)$ necessarily evolves as a stochastic process.

We ultimately will be interested in the statistical properties of the phase error. We may however note that a sample expression for the mean of $\Phi(t)$ in (2-9) can be generated, which may be useful in signal design. If we average both sides of (2-9) and interchange averaging and differentiation on the left, we see that

$$\frac{\partial \bar{\Phi}(t)}{\partial t} = \left[(\omega_s - \omega_0) + \frac{d\theta_1}{dt} \right] - e k \int_{-\infty}^t f(t-\tau) \cdot \left\{ E \cos[\omega_s \tau + \theta_1 - \Phi(\tau)] \sum_{m=1}^N h(\tau - t_m) \right\} d\tau \quad (2-10)$$

where $\bar{\Phi}(t)$ is the mean of $\Phi(t)$. The averaging in the integrand can be carried out by using the conditional expectations:

$$E[\quad] = E_{\Phi} \left\{ E_{t_m, N} | \Phi [\quad] \right\} . \quad (2-11)$$

The inner expectation involves only the average of the shot noise, which is given in (1-5) as

$$E \sum_{m=1}^N \delta(t - t_m) = n_s(t) . \quad (2-12)$$

Substitution into (2-11), allows us to rewrite the braces in (2-10) as

$$E_{\Phi} \left\{ \sin[(\omega_0 - \omega_s)t + \Phi] \right\} + E_{\Phi} [\text{terms at } (\omega_0 + \omega_s)] . \quad (2-13)$$

The loop filtering in (2-9) eliminates the sum frequency term. Hence, (2-10) becomes

$$\frac{\partial \bar{\Phi}(t)}{\partial t} = \left[(\omega_s - \omega_0) + \frac{d\theta_1}{dt} \right] - e k \int_{-\infty}^t f(t-\tau) E_{\Phi} \left\{ \sin(\omega_0 - \omega_s) \tau + \Phi(\tau) \right\} d\tau \quad (2-14)$$

The above is interesting in that it shows that if the loop is tracking frequency and phase fairly accurately (i. e., $\omega_s = \omega_0$ and $\sin(\varphi) \approx \varphi$), then (2-14) is approximately

$$\frac{\partial \bar{\Phi}(t)}{\partial t} \approx \frac{d\theta_1}{dt} - e k \int_{-\infty}^t f(t-\tau) \bar{\Phi}(\tau) d\tau . \quad (2-15)$$

This equation has the form of the deterministic tracking error produced in the linear feedback loop shown in Figure 3, when forced by the input $\theta_1(t)$. Note that the equivalent linear loop replaces the VCO by an integrator, the mixer by a subtractor, and retains the same loop filter. Hence, the loop error function in (2-9) has a mean value such that when the loop is tracking well [i. e., $|\Phi(t)| \ll 1$], the mean varies in time according to the error function of the linear system in Figure 3. The latter system can therefore be used to design loop filters and compute mean error performance.

For a complete statistical analysis, however, we must return to (2-9) for study. The complexity of the error process $\Phi(t)$ is exhibited even if we consider a simplified special case. For example, consider a first order loop in which the loop filter is removed. [This effectively replaces $f(t)$ by a delta function in (2-6).] In this case, (2-9) becomes

$$\frac{d\Phi}{dt} = \left[(\omega_s - \omega_0) + \frac{d\theta_1}{dt} \right] - ek \cos[\omega_s t + \theta_1(t) - \Phi(t)] \cdot \sum_{m=1}^{N(0,t)} \delta(t-t_m). \quad (2-16)$$

Though simplified, (2-16) is still a non-linear differential equation involving the random loop error process $\Phi(t)$. By integrating both sides we note

$$\Phi(t) = [(\omega_s - \omega_0)t + \theta_1(t)] - ek \sum_{m=1}^{N(0,t)} \cos[\omega_s t_m + \theta_1(t_m) - \Phi(t_m)]. \quad (2-17)$$

The second term represents a summation of random "jumps", the height of the jumps dependent upon $\Phi(t)$ itself. This identifies the process $\Phi(t)$ in (2-16) as a discontinuous, or "jump", process in which the

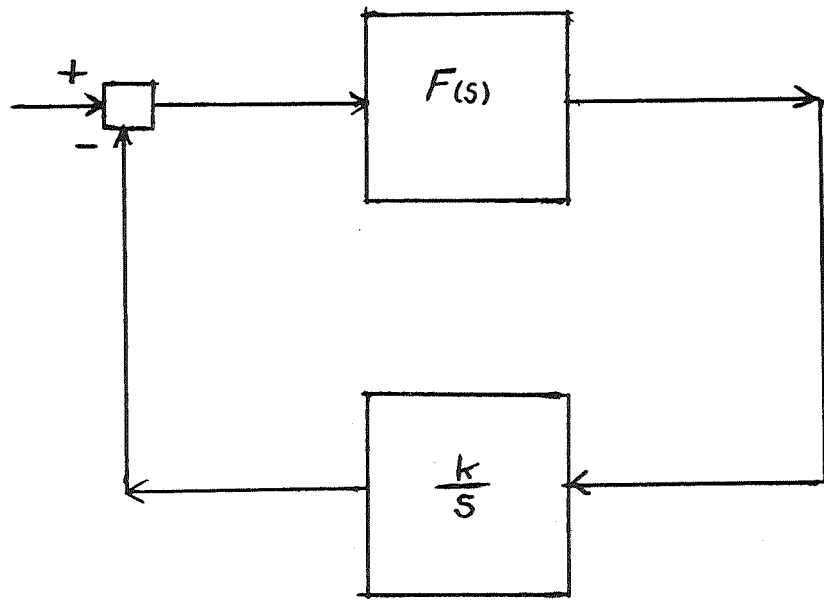


Figure 3

number of jumps are governed by the counting process $N(0, t)$. Therefore, even for this specialized case, the complexity of the error process is apparent.

In the following section we derive an equation involving the probability density of a general random process. Subsequently, we shall apply the result to the error process generated in (2-9).

2.2 Probability Density Equations of Random Processes

Let $\Phi(t)$ be a scalar random process, and let $p(\Phi_1, t_1)$ represent the probability density function (pdf) of the process at time t_1 in the variable Φ_1 . Similarly, denote $p(\Phi_1, t_1 | \Phi_2, t_2)$ as the conditional pdf of $\Phi(t)$ at time t_1 , given that $\Phi(t_2) = \Phi_2$ at time t_2 . The pdf is then always related to the conditional pdf by

$$p(\Phi_1, t_1) = \int_{-\infty}^{\infty} p(\Phi_1, t_1 | \Phi_2, t_2) p(\Phi_2, t_2) d\Phi_2 \quad (2-18)$$

Note that the conditional density can be interpreted as a transitional density in the sense that it "converts" the pdf at time t_2 to its new density at time t_1 . When $t_1 > t_2$, this transitional density essentially indicates the manner in which the pdf propagates in time.

Equation (2-18) can be rewritten in a different form for convenient interpretation and application. Define the conditional characteristic function of the random increment $\Delta\Phi = \Phi_2 - \Phi_1$ as

$$C_{\Delta}(\omega) = \int_{-\infty}^{\infty} e^{j\omega(\Phi_1 - \Phi_2)} p(\Phi_1, t_1 | \Phi_2, t_2) d\Phi_1 \quad (2-19)$$

By inverse Fourier transform

$$p(\Phi_1, t_1 | \Phi_2, t_2) = \frac{1}{2\pi} \int_{-\infty}^{\infty} e^{-j\omega(\Phi_1 - \Phi_2)} C_{\Delta}(\omega) d\omega \quad (2-20)$$

Substitution of (2-20) into (2-18) then yields

$$p(\Phi_1, t_1) = \frac{1}{2\pi} \int_{-\infty}^{\infty} p(\Phi_2, t_2) d\Phi_2 \int_{-\infty}^{\infty} e^{-j\omega(\Phi_1 - \Phi_2)} C_{\Delta}(\omega) d\omega . \quad (2-21)$$

Now it is well known that the characteristic function can be expanded into moments as

$$C_{\Delta}(\omega) = 1 + \sum_{i=1}^{\infty} \frac{(j\omega)^i}{i!} m_i(\Delta\Phi) \quad (2-22)$$

where

$$m_i(\Delta\Phi) = E_{\Phi_1} [(\Phi_1 - \Phi_2)^i | \Phi_2] \quad (2-23)$$

is the i^{th} conditional moment of $\Delta\Phi$ given $\Phi(t_2) = \Phi_2$. [Alternatively, $m_i(\Delta\Phi)$ are the moments of the conditional pdf in (2-20).] It follows that

$$p(\Phi_1, t_1) = \sum_{i=0}^{\infty} \frac{1}{2\pi i!} \int_{-\infty}^{\infty} p(\Phi_2, t_2) d\Phi_2 \int_{-\infty}^{\infty} m_i(\Delta\Phi) e^{-j\omega(\Phi_1 - \Phi_2)} (j\omega)^i d\omega . \quad (2-24)$$

But

$$\begin{aligned} \frac{1}{2\pi} \int_{-\infty}^{\infty} e^{-j\omega(\Phi_1 - \Phi_2)} (j\omega)^i d\omega &= \left(-\frac{\partial}{\partial \Phi_1} \right)^i \int_{-\infty}^{\infty} e^{-j\omega(\Phi_1 - \Phi_2)} d\omega \\ &= \left(\frac{\partial}{\partial \Phi_1} \right)^i \delta(\Phi_1 - \Phi_2) \end{aligned} \quad (2-25)$$

and (2-24) becomes

$$\begin{aligned}
p(\Phi_1, t_1) &= \sum_{i=0}^{\infty} \frac{1}{i!} \int_{-\infty}^{\infty} m_i(\Delta\Phi) \left(-\frac{\partial}{\partial\Phi_1}\right)^i p(\Phi_2, t_2) \delta(\Phi_1 - \Phi_2) d\Phi_2 \\
&= p(\Phi_1, t_2) + \sum_{i=1}^{\infty} \frac{1}{i!} \left(-\frac{\partial}{\partial\Phi_1}\right)^i m_i(\Delta\Phi) p(\Phi_1, t_2). \quad (2-26)
\end{aligned}$$

The first term is the pdf at time $t = t_2$, and the summation represents the increment in this latter pdf to produce the pdf at $t = t_1$. If we set $t_2 = t$ and $t_1 = t + \Delta t$, then (2-26) becomes

$$p(\Phi_1, t + \Delta t) - p(\Phi_1, t) = \sum_{i=1}^{\infty} \frac{1}{i!} \left(-\frac{\partial}{\partial\Phi_1}\right)^i m_i(\Delta\Phi) p(\Phi_1, t). \quad (2-27)$$

Dividing by Δt and passing to the limit as $\Delta t \rightarrow 0$ we obtain

$$\frac{\partial p(\Phi, t)}{\partial t} = \sum_{i=1}^{\infty} \frac{1}{i!} \left(-\frac{\partial}{\partial\Phi}\right)^i [K_i(\Phi) p(\Phi, t)], \quad (2-28)$$

where

$$K_i(\Phi) = \lim_{\Delta t \rightarrow 0} \left[\frac{E[(\Delta\Phi)^i | \Phi]}{\Delta t} \right]. \quad (2-29)$$

Equation (2-28) is called the stochastic kinetic equation [17], or the Smoluchowski-Komogorov equation [16]. When the coefficients $K_i(\Phi)$ exist, this equation provides a relation that must be satisfied by the pdf of the process $\Phi(t)$. Note that the equation is a partial differential equation with variable coefficients, and involve all orders of derivatives. The remarkable point is that no continuity conditions on $\Phi(t)$ were required, so that the equation is valid whether $\Phi(t)$ is continuous or not. In essence, the integral equation in (2-18) has been replaced by the differential equation in (2-28). Furthermore, while one needs the complete conditional pdf to carry out (2-18), only the moments of this density are needed to derive (2-28).

The principle usefulness of the Smoluchowski equation occurs when only the first few coefficients $K_i(\Phi)$ are non-zero. In particular, if $K_i = 0$, $i \geq 3$, the resulting equation is called the Fokker-Planck equation, and has been extensively studied [1]. The Fokker-Planck equation will arise whenever the random process $\Phi(t)$ is continuous, while discontinuous processes generate all the coefficients in (2-28) [17]. We would expect this latter condition to be true for our process $\Phi(t)$, based upon our earlier discussion of the apparent jump nature of the error function. Equation (2-28) is a partial differential equation of the type

$$\frac{\partial p(\Phi, t)}{\partial t} = L_{\Phi} [p(\Phi, t)] \quad (2-30)$$

where L_{Φ} is a differential operator in Φ . The usual method for solving this type of equation is by separation of variables. In this method it is assumed that

$$p(\Phi, t) = K(t) p(\Phi) \quad (2-31)$$

and a solution is desired that satisfies Equation (2-30) with the appropriate initial conditions. Substitution into Equation (2-30) yields

$$\frac{1}{K(t)} \frac{dK(t)}{dt} = \frac{1}{p(\Phi)} L_{\Phi} [p(\Phi)] . \quad (2-32)$$

Since the left side depends only on t , and the right side only on Φ , they can be equal only if they equal a constant. Thus

$$\begin{aligned} \frac{dK(t)}{dt} &= cK(t) \\ L_{\Phi} [p(\Phi)] &= cp(\Phi) \end{aligned} \quad (2-33)$$

for some c if a solution is to be found by this method. Furthermore, if $\{c_i\}$ is a set of values of c which satisfy the above, then $p(\Phi, t)$ must be of the form

$$p(\Phi, t) = \sum_i B_i(\Phi) e^{-c_i(t)} \quad (2-34)$$

where the $\{B_i(\Phi)\}$ are determined by appropriate initial conditions. Since each term of the sum approaches zero as t goes to infinity for all c_i greater than zero, the steady state solution, $p(\Phi)$ (defined as the limiting form of $p(\Phi, t)$ as $t \rightarrow \infty$), must be due to the value of $c_i = 0$. Therefore, from (2-33), the steady state solution satisfies

$$L_\Phi [p(\Phi)] = 0. \quad (2-35)$$

Thus, the steady state solution to (2-35) (if one exists) is the solution to a differential equation obtained by setting the right hand side of (2-30) equal to zero and replacing $p(\Phi, t)$ by $p(\Phi)$.

2.3 Probability Density Equations of Loop Tracking Errors

It has been shown that a general random process has a probability density which satisfies the Kolmogorov partial differential equation. We have seen that this equation may, however, involve an infinite number of derivative terms. In this section we would like to derive the corresponding pdf equation for the phase error process of a tracking loop, governed by the dynamical equation in (2-9). To accomplish this, we must calculate the sequence of moment coefficients $K_i(\Phi)$ given by (2-29). This in turn requires determinations of the phase increment $\Delta\Phi$ of $\Phi(t)$ during the interval $(t, t + \Delta t)$.

Consider a first order phase lock loop tracking a synchronizing signal with a constant delay, following wideband photo-detection. The phase error $\Phi(t)$ then satisfies the differential equation (2-16), and has the form:

$$\frac{d\Phi}{dt} = ek \cos[\omega_0 t + \theta_1 - \Phi(t)] \cdot \sum_{m=1}^{N(0,t)} \delta(t-t_m) \quad (2-36)$$

where θ_1 is the constant phase delay. Note that the forcing function in (2-15) is zero, so that the steady state mean error is zero. The phase variation $\Delta\Phi$ is obtained by integrating $d\Phi$ from t to $t + \Delta t$. Thus, from (2-16)

$$\begin{aligned} \Delta\Phi &\equiv \int_t^{t+\Delta t} d\Phi = \int_t^{t+\Delta t} \left(\frac{d\Phi}{dt} \right) dt \\ &= -ek \int_t^{t+\Delta t} \cos[\omega_s t + \theta_1 - \Phi(t)] \cdot \sum_{m=1}^{N(0,t)} \delta(t-t_m) dt \\ &= -ek \sum_{m=0}^{N(\Delta t)} \cos[\omega_s t_m + \theta_1 - \Phi(t_m)] \end{aligned} \quad (2-37)$$

where $N(\Delta t)$ is the number of electron occurrences in the interval $(t, t + \Delta t)$. The above expresses the increment of the phase variation during $(t, t + \Delta t)$. Note that this variation is also a "jump process", having randomly occurring "jumps" of random heights, and that the argument of the cosine function depends upon the process $\Phi(t)$ itself (which emphasizes the non-linearity of the loop dynamics).

Now, from Equation (2-29)

$$\begin{aligned}
K_n(\Phi) &= \lim_{\Delta t \rightarrow 0} \frac{1}{\Delta t} E_{N, t_m} [(\Delta\Phi)^n | \Phi] \\
&= \lim_{\Delta t \rightarrow 0} \frac{(-ek)^n}{\Delta t} E_{N, t_m / \Phi} \left[\sum_{m=1}^{N(\Delta t)} \cos^{\theta'}(t_m) \right]^n \quad (2-38)
\end{aligned}$$

where $\theta' = [\omega_0 t + \theta_1 - \Phi]$ and the expectation is conditioned on Φ . The quantity in brackets becomes

$$\sum_{m_1=1}^{N(\Delta t)} \sum_{m_2=1}^{N(\Delta t)} \sum_{m_n=1}^{N(\Delta t)} \cos^{\theta'}(t_{m_1}) \cos^{\theta'}(t_{m_2}) \cdots \cos^{\theta'}(t_{m_n})$$

which is

$$\sum_{m=1}^{N(\Delta t)} \cos^n \theta'(t_m) + \sum_{m_1=1}^{N(\Delta t)} \cdots \sum_{m_n=1}^{N(\Delta t)} \cos^{\theta'}(t_{m_1}) \cdots \cos^{\theta'}(t_{m_n})$$

$$m_1 \neq m_2 \neq \cdots \neq m_n .$$

The expectation over just the second term above is

$$E_{N/\Phi} \left[\sum_{m_1=1}^{N(\Delta t)} \cdots \sum_{m_n=1}^{N(\Delta t)} E_{t_m / N, \Phi} \{ \cos^{\theta'}(t_{m_1}) \cdots \cos^{\theta'}(t_{m_n}) \} \right]$$

$$m_1 \neq m_2 \neq \cdots \neq m_n$$

where $E_{t_m / N, \Phi}$ is a conditional expectation given N and Φ . The expectation over $N(\Delta t)$ simply becomes the average of the counting process over $(t, t + \Delta t)$. Since this expression does not involve those terms where $m_1 = m_2 = \cdots = m_n$, the above expression becomes

$$(\bar{N}^n - \bar{N}) E_{(t_{m_1}, t_{m_2}, \dots, t_{m_n})} [\cos^{\theta'}(t_{m_1}) \cos^{\theta'}(t_{m_2}) \cdots \cos^{\theta'}(t_{m_n})]$$

where from (1-2)

$$\bar{N} = \int_t^{t + \Delta t} n(\tau) d\tau .$$

The conditional expectation of the term in the brackets requires the n-dimensional joint probability density of the n random variables $\{t_m\}$. For Poisson shot noise processes this is obtained from (1-4) as

$$p(t_{m_1}, t_{m_2}, \dots, t_{m_n} | n) = \frac{1}{\bar{N}^n} \prod_{m=1}^n n(t_{m_m}) .$$

Therefore, the conditional expectation over the $\{t_m\}$ is

$$\int_t^{t + \Delta t} \dots \int_{t + t_{m_{n-1}}}^{t + \Delta t} [\cos \theta'(t_{m_1}) \dots \cos \theta'(t_{m_n})] [n(t_{m_1}) \dots n(t_{m_n})] dt_{m_1} \dots dt_{m_n}$$

for $t \leq t_{m_1} \leq \dots \leq t_{m_n} \leq (t + \Delta t)$. As we take the limit as Δt goes to zero this expression behaves as

$$[\cos \theta'(t_{m_1}) \dots \cos \theta'(t_{m_n})] [n(t_{m_1}) \dots n(t_{m_n})] (\Delta t)^n .$$

Therefore, taking the limit as Δt goes to zero the above expression behaves as $(\Delta t)^{n-1}$ which goes to zero. Hence the second term resulting from Equation (2-38) is zero and

$$\begin{aligned} K_n(\Phi) &= \lim_{\Delta t \rightarrow 0} \frac{(-ek)^n}{\Delta t} E_{N, t_m / \Phi} \sum_{m=1}^{N(\Delta t)} \cos^n \theta'(t_m) \\ &= \lim_{\Delta t \rightarrow 0} \frac{(-ek)^n}{\Delta t} \bar{N} E_{t_m / \Phi} [\cos^n \theta'(t_m)] . \end{aligned}$$

The expectation of the bracketed term is

$$\int_t^{t + \Delta t} \cos^n \theta'(t_m) \frac{n(t_m)}{\bar{N}} dt_m$$

and

$$K_n(\Phi) = (-ek)^n \cos^n \theta'(t) n(t). \quad (2-39)$$

This equation represents the general nth conditional moment of the increment of the phase error. Note that it is in terms of the feedback signal and the intensity modulation, $n(t)$. Since Equation (2-39) is basically a product of sinusoids, $K_n(\Phi)$ will contain sine waves at the "beat" frequencies. Remembering that terms involving frequencies of $n\omega_0$, $n \geq 1$, are eliminated by the mixer*, the general expressions for $K_n(\Phi)$ become

$$K_n(\Phi) \begin{cases} -C_n (ek)^n A \sin \Phi & n\text{-odd} \\ C_{n-1} (ek)^n (A) & n\text{-even} \end{cases} \quad (2-40)$$

where

$$C_n = \prod_{i=1}^n \left(\frac{1}{i+1} \right) \quad \begin{matrix} n\text{-odd} \\ i\text{-odd} \end{matrix} \quad (2-41)$$

The series form of the pdf equation now becomes

* Mathematically, we are implying that the expectation operation in Equation (2-29) contains an additional time averaging operation, caused by the filtering effects of the mixer. Thus, to be rigorous, a time averaged version of $K_n(\Phi)$ is being computed.

$$\frac{\partial p(\Phi, t)}{\partial t} = Ab \sum_{\substack{n=1 \\ (n\text{-odd})}}^{\infty} \frac{C_n (ek)^n}{n!} \frac{\partial^n}{\partial \Phi^n} [\sin \Phi p(\Phi, t)] + \\ A \sum_{\substack{n=2 \\ (n\text{-even})}}^{\infty} \frac{C_{n-1} (ek)^n}{n!} \frac{\partial^n p(\Phi, t)}{\partial \Phi^n} . \quad (2-42)$$

The solution to this equation is the pdf, $p(\Phi, t)$, of the phase error, Φ , at each instant of time, t . Note that the equation is an infinite order partial differential equation with coefficients that are functions of the variable Φ . The infinite number of derivative terms can be directly attributed to the "jump" nature of the phase error process. The steady state solution of the pdf is given by (2-35) obtained by setting the right side of (2-42) equal to zero. Thus, with $p(\Phi)$ denoting the steady state pdf, we have

$$0 = Ab \sum_{\substack{n=1 \\ (n\text{-odd})}}^{\infty} \frac{C_n (ek)^n}{n!} \frac{d^n}{d\Phi^n} [\sin \Phi p(\Phi)] + A \sum_{\substack{n=2 \\ (n\text{-even})}}^{\infty} \frac{C_{n-1} (ek)^n}{n!} \frac{d^n p(\Phi)}{d\Phi^n} . \quad (2-44)$$

The steady state pdf can be determined by solving the above total differential equation with the appropriate initial conditions. The equation is still, however, of infinite order and the hope of obtaining an exact solution is somewhat ambitious. Nevertheless, there is still useable information that may be extracted from Equation (2-44) without a complete solution. For example, we note that the coefficients are periodic in Φ , implying that if $p(\Phi)$ is a solution to (2-44) then $p(\Phi + 2\pi)$ is also a solution. Hence, steady state pdf solutions are periodic with period 2π . For this reason we need only concentrate

on deriving a normalized solution over a single period, and Φ will therefore be constrained $(-\pi, \pi)$ in the subsequent analysis. For convenience, we can rewrite (2-44) in a slightly different form by first dividing through by the coefficient for $n = 2$. This yields

$$0 = \alpha \frac{d}{d\Phi} [\sin\Phi p(\Phi)] + \frac{d^2 p(\Phi)}{d\Phi^2} + \left(\frac{1}{2\alpha}\right) \frac{d^3}{d\Phi^3} [\sin\Phi p(\Phi)] \\ + \frac{1}{4\alpha^2} \frac{d^4 p(\Phi)}{d\Phi^4} + \frac{1}{12\alpha^3} \frac{d^5}{d\Phi^5} [\sin\Phi p(\Phi)] \quad (2-45)$$

where $\alpha = 2b/ek$. For a first order loop the gain k is directly related to the loop noise bandwidth B_L by [1]

$$B_L = \frac{eAk}{4} . \quad (2-46)$$

Since it is desirable to operate the loop with a given bandwidth, the loop gain k must be adjusted to achieve this value. Hence, $k = 4B_L/eA$ and the α parameter in (2-45) takes the form

$$\alpha = \frac{Ab}{2B_L} . \quad (2-47)$$

The coefficient Ab can be interpreted as the average rate of electrons of the intensity modulation by the synchronizing signal. In this light, α is then the average number of electrons produced in a $1/2B_L$ time period, i. e., in a time period corresponding to the reciprocal of the designed carrier bandwidth. Hence α can be considered an electron function "density", indicating the accumulation of electron occurrences over a fixed time period. By relating electron occurrences to photons, the density α can also be interpreted in terms of received synchronizing

energy, or in terms of signal to noise ratios. In particular, if we multiply numerator and denominator by $e^2 A$, then

$$\alpha = b \frac{(eA)^2}{e^2 A (2B_L)} \quad (2-48)$$

The term $(eA)^2$ is proportional to the average current power in the synchronizing signal, while $(e^2 A)$ is the spectral level of the shot noise power spectrum and $(e^2 A)2B_L$ is proportional to the total shot noise power in a $2B_L$ bandwidth. Hence, α can also be considered an indication of the signal-to-shot noise power ratio. As such, we would expect performance to improve as α increases. This would mean the modulation index b should be as large as possible for best operation. We shall find this conjecture is true, and therefore from here on b will be given its maximum possible value ($b = 1$) in (2-47).

Note that the higher order coefficients in (2-45) decrease with increasing α . This appears to indicate a diminishing importance of the higher derivative terms in contributing to the solution as α increases. This conjecture will be investigated in the next chapter, and will be shown to have both a mathematical and physical interpretation.

One last point is worthy of comment concerning (2-45). Note that the only parameter effecting the equation, and therefore the solution, is α , the electron (photon) density in a $1/2B_L$ time period. In particular, the synchronizing carrier frequency ω_s in (2-2) does not appear in the solution. Hence, it is meaningless to cite values of numbers of electrons (photons) per cycle of synchronizing carrier frequency in discussing optical time locking. It is

only the number per cycle of loop bandwidth that is significant.
Of course, the sync frequency is important in converting
phase errors in radians to timing errors in seconds.

Chapter 3
PROBABILITY DENSITY SOLUTIONS

In Chapter 2 an infinite order differential equation was derived for the steady state probability density of the loop phase error of a first order tracking loop with shot noise inputs. The equation showed that the coefficients of the resulting derivative terms in the equation depended upon the electron function rate in the photo-detector, which in turn depended upon the received radiation power. In this chapter we investigate approximate solutions for the desired probability density of the tracking error.

3.1 High Electron Density Solution

For the case where the function density α in (2-47) is extremely high, a first approximation to the solution of Eq. (2-45) can be obtained by dropping all terms that have powers of $1/\alpha$ as coefficients. This leads to the equation

$$0 = \alpha \frac{d}{d\Phi} [\sin\Phi p(\Phi)] + \frac{d^2 p(\Phi)}{d\Phi^2} \quad (3-1)$$

where $p(\Phi)$ is the steady state density and α is the electron density at the photo-detector output:

$$\alpha = \frac{A}{2B_L} \quad (3-2)$$

Equation (3-1) is just the steady state form of the Fokker-Planck equation and can easily be solved. Integrating both sides yields

$$C_0 = \alpha \sin \Phi p(\Phi) + \frac{dp(\Phi)}{d(\Phi)} \quad (3-3)$$

where C_0 is an arbitrary constant. This equation can be solved over the interval, $-\pi \leq \Phi \leq \pi$, with the two boundary conditions:

$$1) \quad p(\pi) = p(-\pi) \quad (\text{periodicity})$$

$$2) \quad \int_{-\pi}^{\pi} p(\Phi) d\Phi = 1 .$$

The solution is

$$p(\Phi) = \frac{e^{\alpha \cos \Phi}}{2\pi I_0(\alpha)} \quad (3-4)$$

where I_0 is the imaginary Bessel function. Equation (3-4) is plotted in Figure 4, for various α . Note that the probability density approaches, for large α , a delta function at zero, while for $\alpha \rightarrow 0$, it approaches a uniform density over the phase error interval.

The former case can be considered the limit of perfect tracking, while the latter represents a completely random phase error; i. e., poor phase tracking. The ability to track is therefore directly related to the value of the α parameter.

It is of interest to note that the solution in (3-4) is the same solution obtained for the first order loop when driven by a sinusoidal signal plus additive white Gaussian noise [1, 11]. Thus, the error differential equation due to shot noise inputs becomes identical to that due to additive input Gaussian noise as the higher order coefficients are eliminated. In essence, this serves as an apparent justification for the truncation of Eq. (2-45) to (3-1) for large values of α since it has been shown [3, 5, 6] that a discrete poisson shot noise process approaches a continuous Gaussian process as $\alpha \rightarrow \infty$. Thus, for

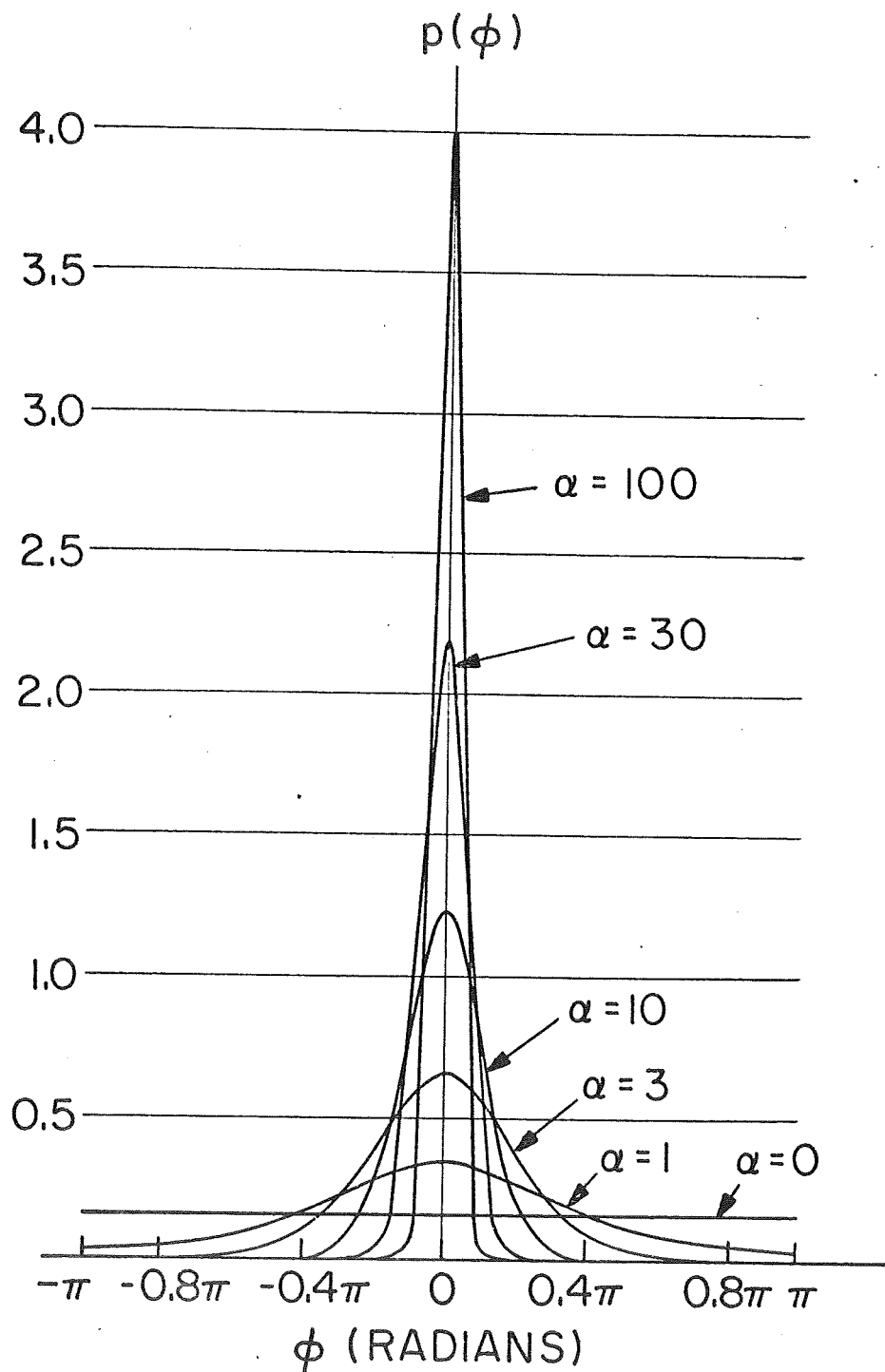


Figure 4.

$\alpha \gg 1$, the shot noise error pdf is, to a first approximation, given by the solution for additive Gaussian noise inputs.

The pdf in (3-4) has zero mean and variance given by

$$\sigma_{\Phi}^2 = \frac{\pi^2}{3} + 4 \sum_{n=1}^{\infty} \frac{(-1)^n I_n(\alpha)}{n^2 I_0(\alpha)} \quad (3-5)$$

where $I_n(\alpha)$ is the nth order imaginary Bessel function. This variance is shown as a function of α^{-1} in Figure 5. As the parameter α approaches zero the variance approaches $\pi^2/3$, the variance of a uniformly distributed random variable over the interval, $(-\pi, \pi)$. It may be seen that the tracking variance for the steady state pdf of the phase error is approximately proportional to $1/\alpha$ for large α . For α below 5, the variance increases rapidly, but the range of validity of the high density solution is questionable.

3.2 High Order Approximations

The density in (3-4) is in theory valid only as $\alpha \rightarrow \infty$. It is not obvious, however, how accurate this solution is for finite α . In this section we investigate higher order truncations of the infinite order equation in (2-45), and the associated solutions, in order to obtain better approximations to the true solution. After integrating (2-45) once with respect to Φ , expanding the derivatives of $\sin \Phi p(\Phi)$, and collecting like derivatives of $p(\Phi)$, we have

$$C_0 = \sum_{n=0}^{\infty} F_n(\Phi) \frac{d^n}{d\Phi^n} p(\Phi) \quad (3-6)$$

Here C_0 is the constant of integration and the $F_n(\Phi)$ functions are of the form

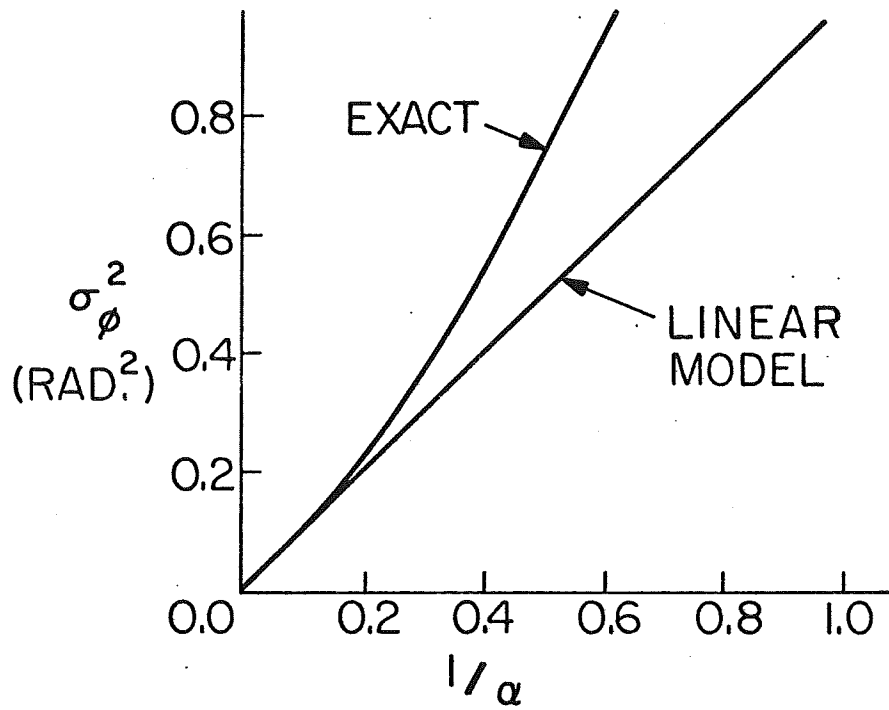


Figure 5.

$$F_0(\Phi) = \sin \Phi \left(\alpha - \frac{1}{2\alpha} + \frac{1}{12\alpha^3} - \frac{1}{144\alpha^5} + \dots \right)$$

$$F_1(\Phi) = 1 + \cos \Phi \left(\frac{1}{\alpha} - \frac{1}{3\alpha^3} + \frac{1}{24\alpha^5} - \dots \right)$$

$$F_2(\Phi) = \sin \Phi \left(\frac{1}{2\alpha} - \frac{1}{2\alpha^3} + \frac{5}{48\alpha^5} - \dots \right)$$

$$F_3(\Phi) = \frac{1}{4\alpha^2} + \cos \Phi \left(\frac{1}{3\alpha^3} - \frac{5}{36\alpha^5} + \dots \right) \quad (3-7)$$

$$F_4(\Phi) = \sin \Phi \left(\frac{1}{12\alpha^3} - \frac{5}{48\alpha^5} + \dots \right)$$

$$F_5(\Phi) = \frac{1}{36\alpha^4} + \cos \Phi \left(\frac{1}{24\alpha^5} - \dots \right)$$

$$F_6(\Phi) = \sin \Phi \left(\frac{1}{144\alpha^5} - \dots \right)$$

etc.

Note that the functions, $F_n(\Phi)$, decrease with α (for $\alpha \geq 1$ and $n \geq 1$) and it is reasonable to assume that solutions to truncations involving higher order terms of Equation (3-7) may yield higher order approximations to the total solution of the finite-order differential equation. The solution to the truncated equation involving terms up to and including the j th derivative of $p(\Phi)$ will be called the j th-order truncation solution. The function, $F_n(\Phi)$, in general involves terms derived from all the odd order derivatives of order $\geq n+1$ in Equation (3-6) operating on $\sin \Phi p(\Phi)$. Therefore, when forming the j th truncated equation from Equation (3-6), the functions $F_n(\Phi)$ must also be appropriately truncated. For example, the solution to the Fokker-Planck equation treated previously may also be called the first-order truncation

solution to Equation (3-6). Since, for a given $\alpha \geq 1$, the functions, $F_n(\Phi)$, decrease in magnitude rapidly with n it is reasonable to expect that solutions (assuming they can be found) to increasingly higher-order truncated equations would also reduce respectively the remainder, when the higher-order truncation solutions are substituted for $p(\Phi)$ in Equation (3-6). This will be examined below as higher-order truncation solutions are found.

A method exists for solving progressively higher-order truncated versions of Equation (3-6). From Ince [14], Boyce and DiPrima [15], and Coddington and Levinson [13] it is shown that the method of Frobenius which assumes a series solution for $p(\Phi)$ of the form

$$p(\Phi) = \Phi^m \sum_{n=0}^{\infty} A_n \Phi^n, \quad A_0 \neq 0 \quad (3-8)$$

is applicable to any-order truncated version of Equation (3-6), even (in theory) the total infinite-order solution. However, to solve exactly, any n th-order truncated equation from Equation (3-6) it is necessary to have $n+1$ boundary conditions (recall C_0 in Equation (3-6) is an unknown constant of integration). In addition to the boundary conditions previously introduced, additional boundary conditions must be specified in order to solve the higher order differential equations.

For the non-offset case, the primary assumption that will be imposed to evaluate the necessary boundary conditions is that the solutions to (3-6) are symmetric about $\Phi = 0$. The solution is therefore an even function about $\Phi = 0$, and between $-\pi$ and π it can be expanded in a Fourier series as an infinite sum of cosines,

$$p(\Phi) = \sum_{n=0}^{\infty} a_n \cos n\Phi \quad (3-9)$$

where the a_n 's are coefficients. From this expression it can be seen that all odd order derivatives of $p(\Phi)$ are zero at $\Phi = 0$ and $\Phi = \pm\pi$. Furthermore, evaluation of the right side of (3-6) at $\Phi = 0$, with this zero condition for the odd derivatives, shows that C_0 is zero. In addition to these initial conditions, we shall further impose the restriction that all even order derivatives, evaluated at $\Phi = \pm\pi$, will be zero also. This results in the set of boundary conditions:

$$\left. \frac{d^n p(\Phi)}{d^n \Phi} \right|_{\pm\pi} = 0, \text{ for all } n \geq 1. \quad (3-10)$$

These conditions, along with the two used in (3-4) will provide a solution to any order truncation of (3-6). In the following sections, solutions to second order and third order truncated equations will be determined.

3.3 Second-Order Truncation Solution

The second-order truncation of Equation (3-6) becomes

$$\frac{\sin \Phi}{2\alpha} p''(\Phi) + \left(1 + \frac{\cos \Phi}{\alpha}\right) p'(\Phi) + \left(\alpha - \frac{1}{2\alpha}\right) \sin \Phi p(\Phi) = 0. \quad (3-11)$$

The point $\Phi = 0$ is a regular singular point of Equation (3-11) and therefore by Theorem 4.3 of Boyce and DiPrima [15] a series solution exists of the form given by Equation (3-8), in either of the intervals $-\rho < \Phi < 0$ or $0 < \Phi < \rho$ where ρ is some positive number. The value of ρ is the radius of convergence of the series in Equation (3-8), and is at least equal to the distance from the origin to the nearest zero of $\sin \Phi / 2\alpha$, which is at π . Hence, a series solution can be found for Φ

in the range $-\pi$ to π for which the series converges.

By writing $\sin\Phi$ and $\cos\Phi$ in their series expansions, substituting Equation (3-8) into Equation (3-11), and collecting like powers of Φ , solutions for m and A_n can be found. Two solutions are found for m , one being zero and the other nonzero. Only the zero value for m yields a non-trivial results and the resulting values for A_n , n even, are

$$A_n = \frac{(-1)^{\frac{n+2}{2}} \sum_{r=0}^{n-2} (-1)^{\frac{r}{2}} \left[\frac{(r-1)r}{(n+1-r)!} + \frac{2r}{(n-r)!} - \frac{\beta}{(n-1-r)!} \right] A_r}{n(\lambda + 1 + n)} \quad (3-12)$$

where $\beta = 2\alpha^2 - 1$, $\lambda = 2\alpha$. A_n , for n odd are all zero since the density is symmetrical. Therefore, for given values of α , all the necessary coefficients, A_n , can be calculated to solve for $p(\Phi)$ in its series expansion. This was carried out on a digital computer for α equal to 1.5, 3, 10, and 30. The right half of the symmetrical density $p(\Phi)$ in (3-8) is plotted in Figures 6, 7, 8, and 9 for these values, along with the solutions to the Fokker-Planck equation for the same α . Note that the truncated solution converges rather quickly to the high density solution, and are practically equivalent for $\alpha \geq 3$. In essence, this can be conjectured as the range of validity of the high density solution. The variance of the phase error, calculated from (3-8), is also shown in Figure 10, along with the variance of the high density solution, Equation (3-5), and that satisfying a linear relation in $1/\alpha$. Again, the results indicate that for $\alpha \geq 2$, the relation in (3-5) is valid for the second order truncation solution as well.

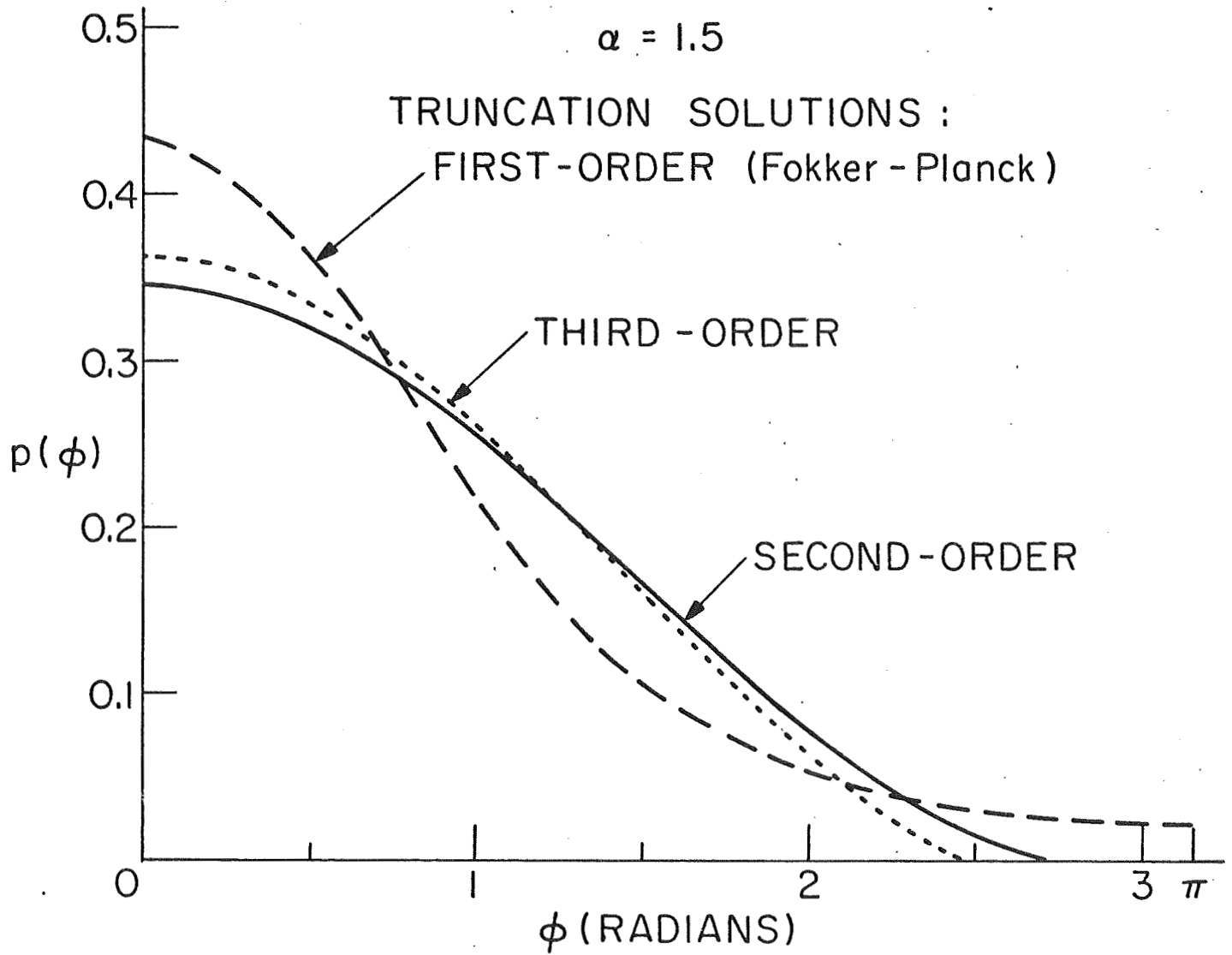


Figure 6.

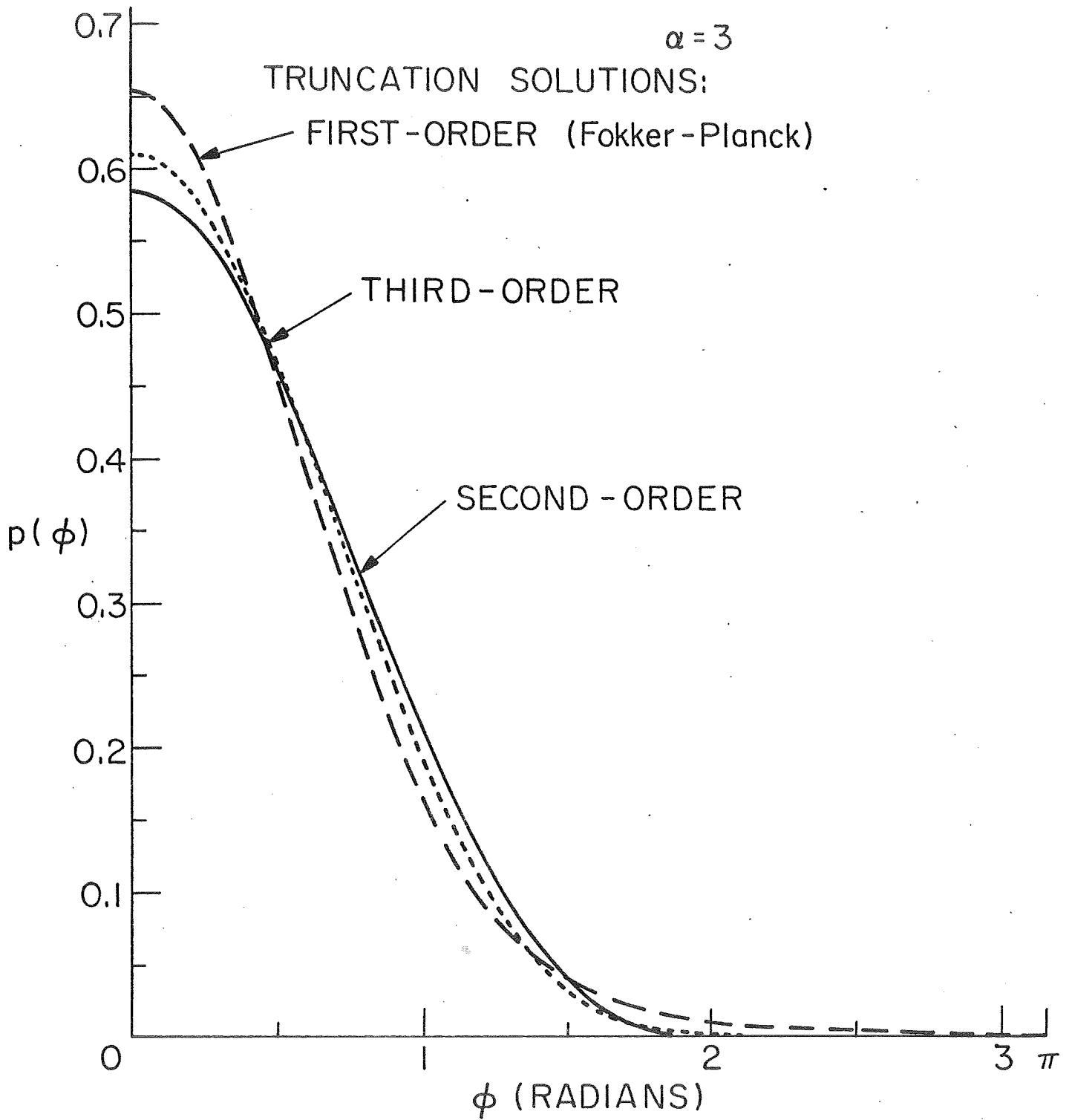


Figure 7.

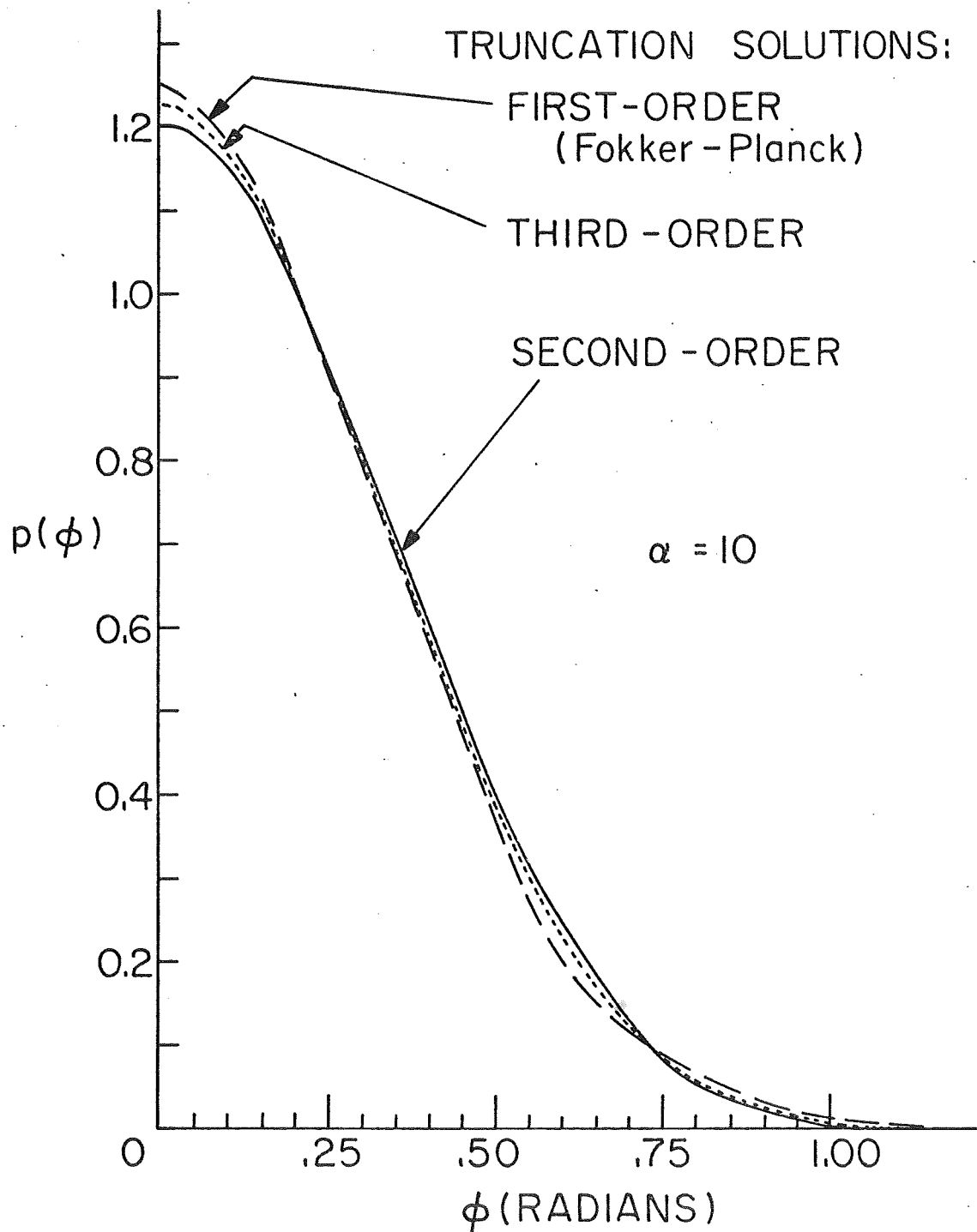


Figure 8.

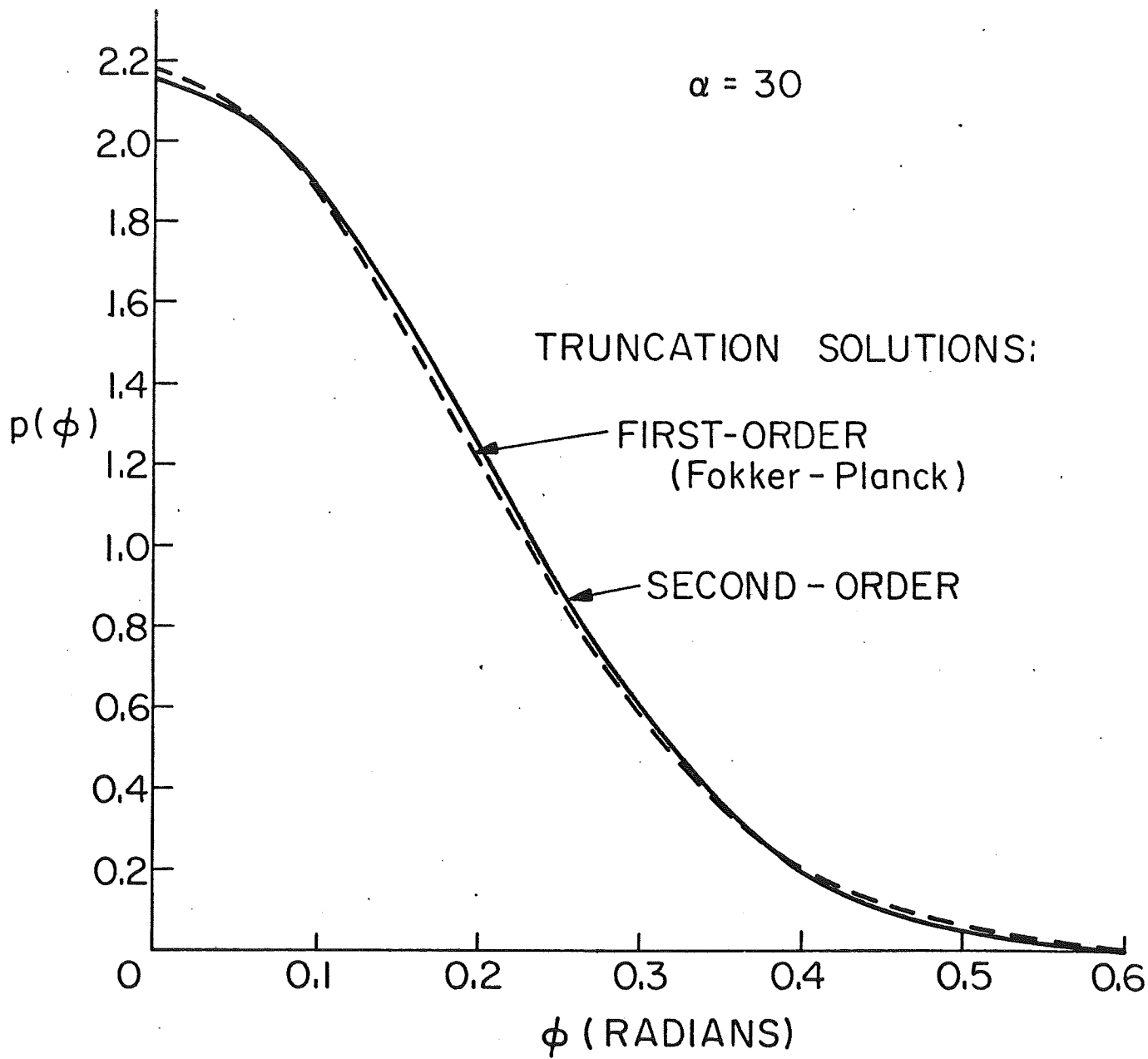


Figure 9.

-40-

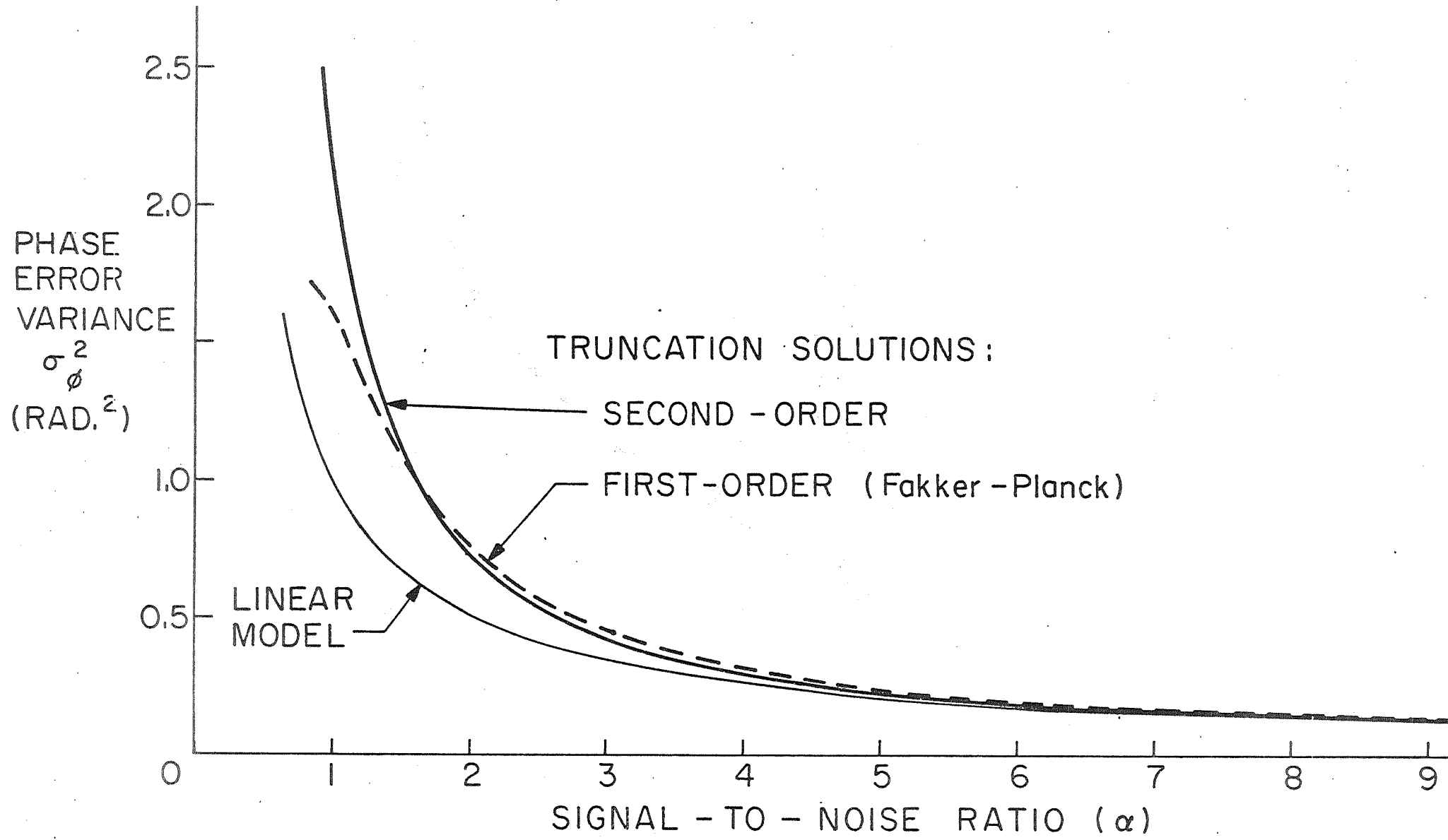


Figure 10.

3.4 Third-Order Truncation Solution

The third-order truncation of Equation (3-6) gives

$$\frac{1}{4\alpha^2} p'''(\Phi) + \frac{\sin\Phi}{2\alpha} p''(\Phi) + \left(1 + \frac{\cos\Phi}{\alpha}\right) p'(\Phi) + \left(\alpha - \frac{1}{2\alpha}\right) \sin\Phi p(\Phi) = 0. \quad (3-13)$$

To solve this equation the previous series method is also used.

However, $\Phi = 0$ is no longer a singular point for this equation, and the series solution is simplified slightly to

$$p(\Phi) = \sum_{n=0}^{\infty} A_n \Phi^n \quad A_0 \neq 0. \quad (3-14)$$

The four boundary conditions used here are

i) $p(\pi) = p(-\pi)$

ii) $\int_{-\pi}^{\pi} p(\Phi) d\Phi = 1$

iii) $p'(\Phi)|_{\pi} = 0$

iv) $p''(\Phi)|_{\pi} = 0.$

Boundary conditions i) and iii) imply all A_n (n-odd) are equal to zero. Use of the same method to determine A_n (n-even) as was used previously, yields the recurrence relation

$$A_n = \frac{\lambda}{n(n-1)(n-2)} \left\{ -[(n-2)(n+\lambda)] A_{n-2} + (-1)^{\frac{n+2}{2}} \sum_{\substack{r=0 \\ (r\text{-even})}}^{n-4} (-1)^{\frac{r}{2}} \left[\frac{-r(r-1)}{(n-r-1)!} - \frac{2r}{(n-r-1)!} + \frac{\beta}{(n-r-3)!} \right] A_r \right\} \quad (3-15)$$

for $n \geq 4$ and $\lambda = 2\alpha$, $\beta = 2\alpha^2_{-1}$. Boundary condition iv) is used to

determine A_2 . Substitution yields

$$\sum_{n=2}^{\infty} n(n-1) A_n \pi^{n-2} = 0. \quad (3-16)$$

Since all the A_n ($n \geq 2$) can be written in terms of A_0 and A_2

Equation (3-16) can be written as

$$\left[\sum_{n=2}^{\infty} n(n-1) \pi^{n-2} D_n \right] A_2 + \left[\sum_{n=4}^N n(n-1) \pi^{n-2} B_n \right] A_0 = 0$$

where D_n and B_n can be determined from Equation (3-15). Then

A_2 is

$$A_2 = - \frac{\left[\sum_{n=4}^N n(n-1) \pi^{n-2} B_n \right]}{\left[\sum_{n=2}^{\infty} n(n-1) \pi^{n-2} D_n \right]} A_0$$

A_0 is then determined by the normalizing boundary condition (ii),

$$\int_{-\pi}^{\pi} p(\Phi) = 1.$$

These computations were also accomplished with a digital computer and the solutions for $p(\Phi)$, $0 \leq \Phi \leq \pi$, are plotted in Figures 6, 7, and 8 for $\alpha = 1.5, 3, \text{ and } 10$, respectively. For $\alpha \geq 1.5$, the third order truncation solution is almost identical to the second order solution.

3.5 Accuracy of the Truncation Solutions

The preceding methods can be used to solve higher-order truncations of Equation (3-6) but the derivation of the expressions for A_n become increasingly more difficult and computer time and size (memory) required increase quite rapidly. Therefore truncation solutions of order higher than three were not attempted. However, it would be of interest to obtain an indication of how well the truncation solutions were approximating the true solution to (2-45). In particular, it is desirable to justify the notion that each succeeding higher-order truncation solution was a better approximation to the total solution. This requires that the truncation solutions be substituted into Equation (3-6), and the magnitude of the remainder associated with the higher order neglected terms should be investigated.

With this objective the solutions obtained for the first-order (Fokker-Planck) and second-order truncations were substituted into Equation (3-6) and the magnitude of the maximum value of the remaining terms were calculated on a computer. The results are plotted in Figure 11 for various values of α . For example, when the first-order solution was used, the largest remainder was due to the second-order term, the next largest due to the third-order term, etc. In addition, the magnitude of the third-order term, when the second-order solution is used, is smaller than it was when the first-order solution was used. It is clear from studying Figure 11 that succeeding higher-order truncation solutions result in smaller remainders, and therefore provide a more accurate approximation to the total solution. Note also that while Figure 11 plots the maximum magnitude of each term, the sign of the remainder terms alternate. Hence, the remainder appears as an

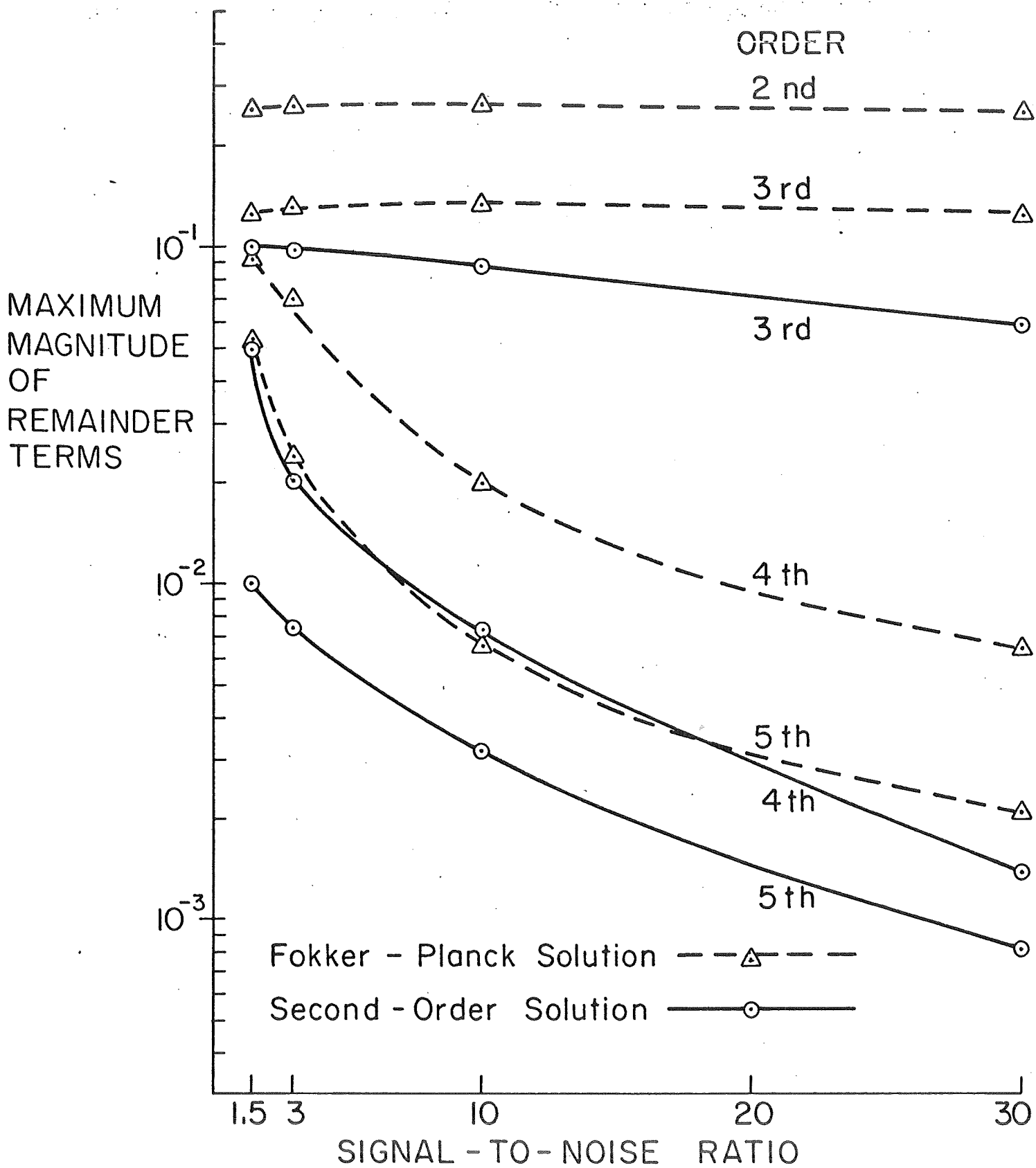


Figure 11.

alternating series of decreasing terms and the magnitude of the remainder for an n th-order solution is bounded by the magnitude of the $n+1$ remainder term. For example, for $\alpha = 10$, the remainder for the Fokker-Planck solution is bounded by the second-order value of 0.26, and the remainder for the second-order solution is bounded by the third-order value of 0.086, down 67%.

From the data presented in Figures 6 through 11 it is indicative that for the low function density case higher-order truncation solutions to Equation (3-6) yield better approximations to the total solution of the infinite-order equation. It is also quite clear that as α increases all the truncation solutions approach the first-order (Fokker-Planck) solution. In other words, the n th-order truncation solution may be represented by

$$p(\Phi) = p_1(\Phi) + p_n^*(\Phi) \quad (3-17)$$

where $p_1(\Phi)$ is the solution to the first-order (Fokker-Planck) equation in (3-4) and $p_n^*(\Phi, \alpha)$ represents the difference between the n th-order and first-order truncation. As α gets very large

$$\lim_{\alpha \rightarrow \infty} p_n^*(\Phi) \rightarrow 0 \quad n > 1$$

and

$$\lim_{\alpha \rightarrow \infty} p_n(\Phi) \rightarrow p_1(\Phi) \quad n > 1$$

The method of solution that has been presented here can reduce this error to as small a number as desired, in theory, given enough time and computer capacity. The third-order truncation solution was the highest-order computed in this analysis and it is shown that this solution is a good compromise in the tradeoff between accuracy and complexity of solution for the range $\alpha \geq 1.5$.

3.6 The VCO Offset Case

It has been assumed that the carrier frequency of the optical modulating signal, ω_s , and the phase-locked-loop VCO rest frequency, ω_0 , have been equal. When this is not the case the VCO offset, $(\omega_s - \omega_0)$, must be included in (2-37). This expression for $\Delta\Phi$ is then modified to

$$\Delta\Phi = (\omega_s - \omega_0) \Delta t - e k \sum_{m=1}^{N(\Delta t)} \cos \theta'(t_m)$$

$$t \leq t_m \leq t + \Delta t \quad . \quad (3-18)$$

The $K_n(\Phi)$ coefficients in the Smoluchowski series equation are modified only through the first one which becomes

$$K_1(\Phi) = (\omega_s - \omega_0) - \frac{1}{2} eAK \sin\Phi \quad .$$

The effect of the VCO offset is such that $p(\Phi)$ is no longer symmetrical. This means that the series method of finding solutions to truncations of the infinite-order Smoluchowski equation now has the odd as well as the even terms in the power series solution for $p(\Phi)$. In addition, the constant C_0 is no longer zero.

As an example of the treatment of the VCO offset case a second-order truncation solution will be found. The pertinent equation is a modified version of (3-11),

$$\frac{\sin\Phi}{2\alpha} p''(\Phi) + \left(1 + \frac{\cos\Phi}{\alpha}\right) p'(\Phi) + \left(\alpha - \frac{1}{2\alpha} - \gamma\right) \sin\Phi p(\Phi) = C_0 \quad (3-19)$$

where

$$\gamma = \frac{8(\omega - \omega_0)}{k^2 (2ne^2 A)} \quad (3-20)$$

is the new parameter due to the offset. For a specific value of γ , (3-19) can be solved by the series method of the previous sections. For example, with $\gamma = (.707)\alpha$, the A_n coefficients in the series solution become

$$A_1 = \frac{\lambda C_0 + .3535 \lambda^2 A_0}{\lambda + 2}$$

$$A_n \text{ (n-even)} = \frac{.3535 \lambda^2 A_{n-1} + (-1)^{\frac{n+2}{2}} \sum_{r=0}^{n-2} (-1)^{\frac{r}{2}} \left[\frac{(r-1)r}{(n-r+1)!} + \frac{2r}{(n-r)!} - \frac{\beta}{(n-r-1)!} \right] A_r}{n(n + \lambda + 1)}$$

$$A_n \text{ (n-odd)} = \frac{.3535 \lambda^2 A_{n-1} + (-1)^{\frac{n+3}{2}} \sum_{r=1}^{n-2} (-1)^{\frac{r+1}{2}} \left[\frac{(r-1)r}{(n-r+1)!} + \frac{2r}{(n-r)!} - \frac{\beta}{(n-r-1)!} \right] A_r}{n(n + \lambda + 1)}$$

where $\lambda = 2\alpha$ and $\beta = 2\alpha^2 - 1$. The two unknown constants, C_0 and A_0 , can be evaluated by using the two boundary conditions

- i) $p(\pi) = p(-\pi)$
- ii) $\int_{-\pi}^{\pi} p(\phi) d\phi = 1.$

This was accomplished on a digital computer for $\alpha = 1.5$ and 3 and the results are plotted in Figure 12 along with the first-order solution for $\alpha = 3$. The obvious difference between this case and the non-offset

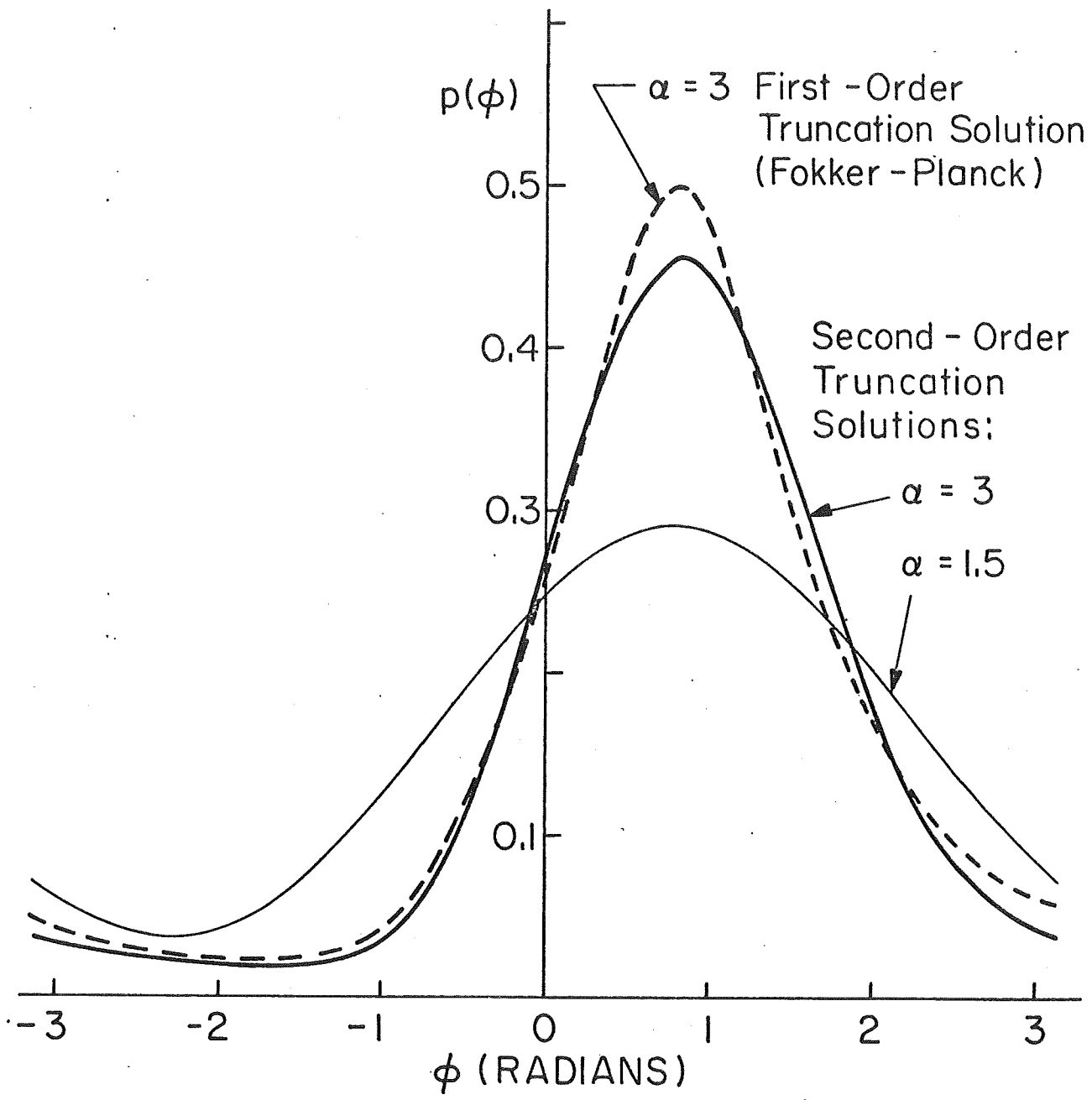


Figure 12.

case is that the peak of the probability density has now shifted from the $\bar{\Phi} = 0$ center line.

The two solutions for $\alpha = 3$ show approximately the same relationship as in Figure 8 for the non-offset case.

Higher-order solutions can also be obtained as in previous sections for the non-offset cases if additional boundary conditions are imposed to evaluate all the unknown constants of integration. The equivalent order offset solution, however, is obtained with more difficulty and complexity than in the non-offset case because C_0 is no longer zero.

Chapter 4

THERMAL NOISE AND PHOTOMULTIPLIERS EFFECTS

In the previous chapters a first order phase locked loop driven by a shot noise process was considered. In this chapter we investigate the effects of additive thermal noise and photomultiplier devices preceeding the loop.

4.1 Additive Gaussian Thermal Noise

Let $r(t)$ represent a zero mean stationary Gaussian noise process having a flat one-sided power spectral density of N_0 watts/hz. When $r(t)$ is added to the shot noise input process of the phase lock loop of Figure (1-2), the output of the loop filter [previously (2-6)] is now

$$e(t) = k_1 \int_0^t f(t-\tau) \left[\sum_{m=1}^{N(t, \tau)} e^{-\delta(\tau - \tau_m)} \cos \theta^1(\tau) + r'(\tau) \right] d\tau \quad (4-1)$$

where $r'(t)$ is the "low frequency" equivalent noise process obtained by mixing the input noise $r(t)$ with the VCO process. It has been shown [1] that the new noise term is itself Gaussian, zero mean, with spectral density given by N_0 ; (i. e., $r'(t)$ is simply a "frequency shifted" version of $r(t)$).

When the transmitted phase variation, $\theta_1(t)$, is a constant, the phase error derivative for the first-order loop has the form

$$\frac{d\Phi}{dt} = -k_e \left[\sum_{m=1}^{N(t)} \delta(t-t_m) \cos \theta^1(t) + r'(t) \right]. \quad (4-2)$$

If this equation is integrated from t to $t + \Delta t$, the incremental phase error becomes

$$\Delta\Phi = ek \sum_{m=1}^{N(\Delta t)} \cos\theta'(t_m) - k \int_t^{t+\Delta t} r'(\tau) d\tau \quad (4-3)$$

The first term is identical to that previously derived in (2-37). The second term accounts for the added effect of the thermal noise. The coefficients of the Smoluchowski equation can now be recalculated for $\Delta\Phi$ of Equation (4-3). In particular, $K_1(\Phi)$ remains the same as before:

$$K_1(\Phi) = -e \frac{Ak}{2} \sin\Phi \quad (4-4)$$

since the expected value of the Gaussian process is zero. The second moment requires calculation of

$$E \left[-ek \sum_{m=1}^{N(\Delta t)} \cos\theta'(t_m) - k \int_t^{t+\Delta t} r'(\tau) d\tau \right]^2 \quad (4-5)$$

The expectation of the square of the first term has previously been calculated, the expectation of the cross term is zero, and the expectation of the square of the second term is $k^2 N_0/2$. Therefore

$$K_2(\Phi) = \frac{k^2}{2} [e^2 A + N_0] \quad (4-6)$$

For computing the higher amounts, $A_n(\Phi)$, define

$$P = e \sum_{m=1}^{N(\Delta t)} \cos\theta'(t_m)$$

$$G = \int_t^{t+\Delta t} r'(\tau) d\tau.$$

Then,

$$E[P + G]^n = E(P^n + a_{n-1} P^{n-1} G + a_{n-2} P^{n-2} G^2 + a_{n-3} P^{n-3} G^3 + \dots).$$

Since the Poisson and Gaussian processes are independent, this becomes

$$E[P+G]^n = [EP^{n-1} + a_{n-1} E(P^{n-1}) E(G) + a_{n-2} E(P^{n-2}) E(G^2) + \dots] .$$

It has been shown [1] that for

$$\lim_{\Delta t \rightarrow 0} \frac{1}{\Delta t} E(G^n) = 0 \quad n > 2 .$$

The expectation of P^{n-m} has already been calculated in (2-33) and been found proportional to Δt . Thus

$$\lim_{\Delta t \rightarrow 0} \frac{1}{\Delta t} a_{n-2} E(P^{n-m}) E(G^m) = 0 \quad \begin{matrix} n \geq 2 \\ m \geq 1 \end{matrix}$$

and therefore,

$$K_n(\Phi) = \lim_{\Delta t \rightarrow 0} \frac{(-k)^n}{\Delta t} E(P^n) \quad n > 2 \quad (4-7)$$

which is the same as in the earlier section when no additive Gaussian noise was present. Hence, the Smoluchowski series equation has been modified only in the second term, $K_2(\Phi)$. The solution for the probability density of the phase error again requires solution of (2-45) with the appropriate K_2 modification. It has already been shown that an excellent approximate solution for the high α case is the solution to the Fokker-Planck equation. For the new $K_2(\Phi)$ term this becomes

$$P(\Phi) \approx \frac{e^{\alpha \cos \Phi}}{2\pi I_0(\alpha)} \quad (4-8)$$

with the parameter α is redefined as

$$\alpha = \frac{\frac{1}{2} (eA)^2}{B_L [e^2 A + N_0]} \quad (4-9)$$

Note that the parameter α now takes on a slightly different meaning. The bracketed denominator term is the sum of the spectral level due to the shot noise and the spectral level of the additive Gaussian noise. Hence, the denominator represents the total effective noise in the $2B_L$ loop bandwidth, due to both the shot noise and additive noise. The numerator is the average power of the intensity process. Thus, α now plays the role of an operating signal-to-noise power ratio in the tracking loop bandwidth. The dependence of $p(\Phi)$ in (4-8) on α had been shown earlier in Figure 4, and the results there are valid with above interpretation of α .

Effect of Photomultiplication

In many optical systems photomultiplication is used at the photodetector to enhance the received signal. The objective of this section is to investigate the effects of photomultiplication on the behavior of the phase error in a first-order tracking system.

An ideal photomultiplication of gain G has the property that it produces G electrons at the photodetector output for each photo-electron at the input. If the electrons are considered identical this has the effect of producing an equivalent electron pulse waveform whose magnitude is G times the magnitude of a single electron pulse waveform. Effectively, this increases the charge of a single electron by the gain G . The shot noise current of Equation (2-1) may then be written as

$$x(t) = \sum_{m=1}^{N(t)} (eG) \delta(t-t_m) . \quad (4-10)$$

The pdf for the phase error in the high function density case is again given by (3-4), where the signal to noise ratio parameter α is now

$$\alpha = \frac{\frac{1}{2} (eGA)^2}{B_L [(eG)^2 A + N_0]} \quad (4-11)$$

and B_L is now $eGAk/4$. The photomultiplication advantage is easily seen when the additive noise term of power spectrum level N_0 is dominant. In this case an increase in the α parameter can be achieved by increasing the photomultiplication gain G .

In the practical fabrication of photomultipliers the gain itself is often a random variable. In the following it is assumed that the photomultiplier has a statistically variable gain which is a random variable with mean \bar{G} and mean square $\overline{G^2}$. This means that each electron at the input produces G electrons at the output, where G is a positive random variable. The shot noise current now becomes

$$x(t) = \sum_{m=1}^{N(t)} eG_m \delta(t-t_m) \quad (4-12)$$

where the $\{G_m\}$ constitutes a set of random variables, independent, and identically distributed over zero to infinity. The incremental change in the process is now

$$\Delta\phi = -ek \sum_{m=1}^{N(\Delta t)} G_m \cos \theta'(t_m) - k \int_t^{t+\Delta t} r'(\tau) d\tau$$

and the first two moments become

$$K_1(\Phi) = - \frac{ek \bar{G} A}{2} \sin \Phi$$

$$K_2(\Phi) = \frac{k^2}{2} [(ek)^2 \overline{G^2}(A) + N_0] .$$

The signal-to-noise ratio α is modified to

$$\alpha = \frac{\frac{1}{2} (e\bar{G}A)^2}{B_L [e^2 \overline{G^2} A + N_0]} \quad (4-12)$$

with

$$B_L = e \frac{\bar{G}AK}{4} .$$

Hence, the shot noise power spectrum is increased by the mean square of the gain, while the signal power is increased by the square of the mean gain.

In some analyses it is common to assume the random gain is Gaussian with a mean \bar{G} , and a standard deviation, or "spread", given as a fraction of the mean gain. That is,

$$\sigma_G = \rho \frac{\bar{G}}{2} \quad 0 \leq \rho \leq 1 .$$

In this case the mean square gain is

$$\overline{G^2} = (\bar{G})^2 \left(1 + \frac{\rho^2}{4} \right) \quad 0 \leq \rho \leq 1$$

and Equation (2-41) becomes

$$\alpha = \frac{\frac{1}{2} (e\bar{G}A)^2}{B_L [e^2(\bar{G})^2 (1 + \frac{\rho^2}{4})A + N_0]}$$

Note that the α parameter degrades as the "spread" parameter ρ increases.

Chapter 5
SECOND-ORDER LOOP ANALYSIS AND
THE GENERAL TRACKING LOOPS

In this chapter the analysis of phase-locked-loops with shot noise inputs is extended to loops of order greater than one, and to the first-order loop where the input and feedback functions are not necessarily sinusoidal (general tracking loops). For the second-order loop a vector form of the Smoluchowski equation is used for the phase error probability density, and solution can be approximated under conditions similar to those of the first-order loop. For the general tracking loop, a generalized Smoluchowski equation for the probability density is used, and again can be solved by the numerical techniques presented in Chapter 3.

5.1 The Two Dimensional Smoluchowski Equation

The Smoluchowski-Kolmogorov probability density equation was derived in Chapter 2 for a general scalar random process $\Phi(t)$. The same basic procedure can be repeated for a vector random process, and a similar vector form of (2-28) will result. Specifically, if we denote

$$\underline{\Phi}(t) = \{\Phi_1(t), \Phi_2(t)\} \quad (5-1)$$

as the two dimensional vector process having scalar random component processes $\{\Phi_i(t)\}$, then the vector equivalent of (2-18) is

$$P(\underline{\Phi}_1, t_1) = \int P(\underline{\Phi}_1, t_1 | \underline{\Phi}_2, t_2) P(\underline{\Phi}_2, t_2) d\underline{\Phi}_2 \quad (5-2)$$

where $\underline{\Phi}_i = \{\Phi_1(t_i), \Phi_2(t_i)\}$. Defining the two dimensional equivalent

of the characteristic function in (2-19), and repeating the steps in (2-20) through (2-28) will yield the equation

$$\frac{\partial P(\underline{\Phi}, t)}{\partial t} = \sum_m \sum_n \frac{(-1)^{m+n}}{m!n!} \frac{\partial^{m+n}}{\partial \Phi_1^m \partial \Phi_2^n} [K_{mn}(\underline{\Phi}) P(\underline{\Phi}, t)] \quad (5-3)$$

where

$$K_{mn}(\underline{\Phi}) = \lim_{\Delta t \rightarrow 0} \frac{E[(\Delta \Phi_1)^m (\Delta \Phi_2)^n]}{\Delta t} \quad (5-4)$$

Equation (5-3) is just the two dimensional equivalent of the Smoluchowski equation in (2-28). Note that evaluation of the coefficients $\{K_{mn}\}$ require all the statistical cross-moments of the joint variations $\Delta \Phi_1$ and $\Delta \Phi_2$ in the components of the process $\underline{\Phi}(t)$. In the following section we apply (5-3) to a second order phase lock tracking loop.

5.2 Second Order Phase Lock Loops

A second order phase lock loop is one in which the loop filter in Figure 2 introduces an integration. The basic form of such a filter would be one having transfer function

$$F(s) = \frac{s+a}{s} = 1 + \frac{a}{s} \quad (5-5)$$

where a represents a possible zero of transmission. The impulse response corresponding to (5-5) is then

$$f(t) = \delta(t) + a \quad .$$

For a shot noise input, the general loop error dynamical equation in (2-9) now becomes

$$\frac{d\Phi(t)}{dt} = -ek \cos \theta'(t) \sum_{m=1}^{N(t)} \delta(t-t_m) - aek \sum_{m=1}^{N(t)} \cos \theta'(t_m). \quad (5-6)$$

We now see that the variation $\Delta\Phi$ will contain a term in Φ [as in (2-37)] and a term involving an integral in Φ , due to the second term in (5-6). It is therefore convenient to define the vector

$$\underline{y}(t) = \{y_0(t), y_1(t)\} \quad (5-7)$$

where

$$y_1(t) = \frac{dy_0(t)}{dt} \quad (5-8)$$

and let

$$\Phi(\tau) = y_0(t) + y_1(t) . \quad (5-9)$$

That is, we consider the error process in (5-6) to be decomposed into the sum of the components of a vector process $\underline{y}(t)$. The probability density of $\Phi(t)$ is then determined from the joint probability density $P(\underline{y}, t)$ by the relation

$$P(\Phi, t) = \int [P(\underline{y}, t)]_{y_0 = \Phi - y_1} dy_1 . \quad (5-10)$$

Substitution of (5-8) and (5-9) into (5-6) yields

$$\begin{aligned} a \frac{dy_0(t)}{dt} + aek \sum_{m=1}^{N(t)} \cos \theta'(\bar{y}, t_m) + \\ \frac{dy_1(t)}{dt} + ek \cos \theta'(\bar{y}, t) \sum_{m=1}^{N(t)} \delta(t-t_m) = 0 \end{aligned} \quad (5-11)$$

where the dependence of $\theta'(t)$ on $\bar{y}(t)$ is emphasized. The above may be decomposed into the two equations

$$a \frac{dy_0(t)}{dt} + aek \sum_{m=1}^{N(t)} \cos \theta'(\bar{y}, t_m) = 0$$

$$\frac{dy_1(t)}{dt} + ek \cos \theta'(\bar{y}, t) \sum_{m=1}^{N(t)} \delta(t-t_m) = 0$$

where it is noted that the second equation is simply the derivative of the first. The above two equations may therefore be represented by the two first-order differential equations:

$$\frac{dy_0(t)}{dt} = y_1(t) \quad (5-12a)$$

$$\frac{dy_1(t)}{dt} = -ek \cos \theta'(\bar{y}, t) \sum_{m=1}^{N(t)} \delta(t-t_m) \quad (5-12b)$$

The above equations specify the dynamics of the vector process $y(t)$ corresponding to (5-9). It is therefore possible to determine the equation for the joint density $P(\underline{y}, t)$ in (5-10) by using the two dimensional Smoluchowski in (5-3). The increments of the vector components given in (5-12) are

$$\Delta y_0 = y_1(t) \Delta t \quad (5-13a)$$

$$\begin{aligned} \Delta y_1 &= -ek \int_t^{t+\Delta t} \cos \theta'(\bar{y}, \tau) \sum_{m=1}^{N(\tau)} \delta(\tau - \tau_m) d\tau \\ &= -ek \sum_{m=1}^{N(\Delta t)} \cos \theta'(\bar{y}, t_m) \end{aligned} \quad (5-13b)$$

These increments are needed to calculate the joint moments, $K_{mn}(y_0, y_1)$ given by Equation (5-4). The $K_{mn}(y_0, y_1)$ are calculated to be

$$K_{10}(\bar{y}) = y_1$$

$$K_{01}(\bar{y}) = -\frac{ekA}{2} \sin(y_0 + y_1)$$

$$K_{02}(\bar{y}) = (ek)^2 (A)/2$$

$$K_{on}(\bar{y}) = (-ek)^n \cos^n \theta'(\bar{y}, t) n(t, \theta) \quad n \geq 3$$

where again

$$n(t, \theta) = A + A \sin[\omega_s t + \theta_1(t)] .$$

All the other $K_{mn}(\bar{y})$ moments not listed above are zero. In this case the two-dimensional Smoluchowski series equation becomes

$$\begin{aligned} \frac{\partial p(\bar{y})}{\partial t} = & -y_1 \frac{\partial p(\bar{y})}{\partial y_0} + \frac{\partial}{\partial y_1} \left[\frac{ekA}{2} \sin(y_0 + y_1) p(\bar{y}) \right] \\ & + n \frac{(ek)^2 A}{4} \frac{\partial^2 p(\bar{y})}{\partial y_1^2} \\ & + \sum_{n \geq 3}^{\infty} \frac{(-1)^n}{n!} \frac{\partial^n}{\partial y_1^n} [K_{on} p(\bar{y})] . \end{aligned} \quad (5-14)$$

The above again represents an infinite order partial differential equation for the joint density $P(\underline{y}) \equiv P(\underline{y}, t)$. Some simplicity is afforded by considering only the steady state solution, but the resulting equation is still difficult to solve explicitly without digital computation.

For the case where the average intensity A is much greater than the loop bandwidth B_L (i. e., large electron density) the approximate steady state solution to (5-14) can be found by limiting the number of terms involved. The corresponding steady state solution for $\Phi(t)$ from (5-10) is then approximately,

$$P(\Phi) \approx \frac{e^{\alpha \cos \Phi}}{2\pi I_0(\alpha)} \quad A \gg B_L \quad (5-15)$$

where $\alpha = A/2B_L$, but B_L now has the definition

$$B_L = \frac{eAk + 2a}{4} \quad (5-16)$$

That is, the loop bandwidth B_L is increased by the added zero in the loop filter of (5-1). The high density solution for $P(\Phi)$ is therefore identical to that of the first order loop case, with the adjustment in the B_L bandwidth. For higher-order loops an equivalent n-dimensional vector process must be defined and an n-dimensional Smoluchowski equation must be derived, increasing the complexity of the problem.

5.3 General Delay Tracking Loops

The objective of this section is to investigate the behavior of a phase tracking system when the input intensity modulation signal and loop feedback function are to a general periodic nature, but not necessarily sinusoidal. Let the signal electron rate of Equation (2-2) be represented by $n_s(t, \tau_1(t))$ and the feedback function by $y(t, \tau_2(t))$ where $\tau_1(t)$ and $\tau_2(t)$ are their respective time delays. The differential equation describing the loop operation for shot noise inputs, where θ_1 is again assumed constant, becomes

$$\frac{d\tau(t)}{dt} = -ek \sum_{m=1}^{N(t)} \delta(t-t_m) y(t, \tau_2(t)) \quad (5-17)$$

where $\tau(t) = \tau_1(t) - \tau_2(t)$ and $N(t)$ is again a Poisson random variable with intensity $n_s(t, \tau_1(t))$. The incremental delay error is

$$\Delta\tau = -ek \sum_{m=1}^{N(\Delta t)} y(t_m, \tau_2(t_m)) \quad (5-18)$$

and the $K_n(\tau)$ moments of the Smoluchowski series equation are now

$$K_n(\tau) = \lim_{\Delta t \rightarrow 0} \frac{1}{\Delta t} E \left[-ek \sum_{m=1}^{N(\Delta t)} y(t_m, \tau_2(t_m)) \right] \quad (5-19)$$

where the expectation is conditioned on τ . Thus, Equation (5-19) becomes

$$K_n(\Phi) = (ek)^n \overline{y^n(t, \tau_2(t)) n(t, \tau_1)} \quad (5-20)$$

where the over-bar represents time averaging inherent in the loop mixer function. Hence, $K_n(\Phi)$ is of the same form as in Equation (2-39), and would be identical to it if

$$\begin{aligned} n(t, \tau_1) &= A + A \sin(\omega_0 t + \tau_1) \\ y(t, \tau_2(t)) &= \partial n(t, \theta) / \partial \theta \\ &= \cos(\omega_0 t + \tau_2(t)) . \end{aligned}$$

The third-order truncated Smoluchowski series equation* for a general input function becomes

$$\begin{aligned} \frac{\partial p(\tau, t)}{\partial t} &= ek \frac{\partial}{\partial \tau} \left[\overline{y(t, \tau_2(t)) n(t, \tau_1)} p(\tau, t) \right] + \frac{(ek)^2 \delta^2}{2 \partial \tau^2} \\ &\quad \left[\overline{y^2(t, \tau_2(t)) n(t, \tau_1)} p(\tau, t) \right] + (ek)^3 \frac{\partial^3}{\partial \tau^3} \left[\overline{y^3(t, \tau_2(t)) n(t, \tau_1)} p(\tau, t) \right] \end{aligned} \quad (5-21)$$

* Here, attention is restricted again to only the first three terms of the infinite series equation, accepting the results as only an approximate solution.

The steady state version of Equation (5-21) occurs when the left-hand side is zero. Integrating the equation with respect to τ gives

$$C_0 = ek[R_{yn}(\tau) p(\tau)] + n \frac{(ek)^2}{2} \frac{d}{d\tau} [R_{y2n}(\tau)] + (ek)^3 \frac{d^2}{d\tau^2} [R_{y3n}(\tau) p(\tau)] \quad (5-22)$$

where

$$R_{yn}(\tau) = \overline{yn}$$

$$R_{y2n}(\tau) = \overline{y^2n}$$

$$R_{y3n}(\tau) = \overline{y^3n}$$

are correlation functions. Note that this equation corresponds to the previously considered equation (2-45) with the sinusoidal functions replaced by the general time averaged correlation functions given above.

5.4 An Example—Early Late Gate Tracking

In radar and pulse tracking systems a periodic pulse train is locked to a locally generated periodic signal through a feedback tracking system, similar to that in Figure 2. When the two signals are in time lock, the local signal tracks the time variations in the arrival times of the incoming periodic pulse train. In optical tracking systems the pulse train is generated by a pulsed laser whose intensity is detected by a photodetector at the receiver. The feedback signal in the tracking loop is designed such that when it is multiplied with the detected pulse train and integrated over some period the result is an error function that is odd with respect to the time delay. This local signal is often designed

to be a periodic train of positive-negative pulses as in Figure 13. The multiplication of the received pulse train by this particular local signal is equivalent to "gating in" the former signal by the latter signal. Hence, the receiver is often called an "early late gate" or "split-gate" tracker.

Since the output of a photodetector is a shot noise process with intensity $n(t, \tau_1)$, the analysis problem is an example of the application of the general tracking theory of the previous section. By referring to Figure 13 it is easily seen that

$$y^3(t, \tau_2(t)) = y(t, \tau_2(t))$$

$$y^2(t, \tau_2(t)) = \frac{1}{2A} [n(t, \tau_2(t))]$$

and therefore

$$R_{yn}(\tau) \equiv \overline{y(t, \tau_2(t)) n(t, \tau_1)} = \overline{y^3(t, \tau_2(t)) n(t, \tau_1)}$$

$$= R_{y^3 n}(\tau)$$

$$= \frac{1}{T} \int_0^T y(t, \tau_2(t)) n(t, \tau_1) dt \quad (5-23)$$

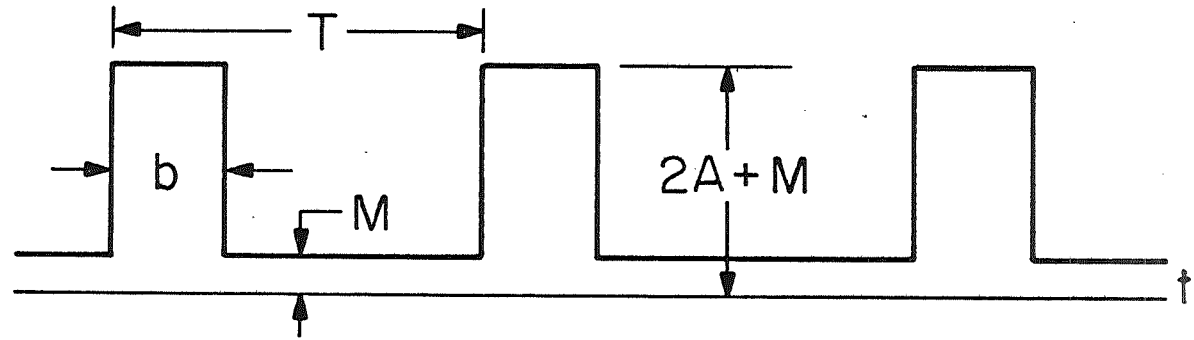
$$R_{nn} \equiv \overline{y^2(t, \tau_2(t)) n(t, \tau_1)}$$

$$= \frac{1}{2AT} \int_0^T n(t, \tau_2(t)) n(t, \tau_1) dt + (\text{a constant}) . \quad (5-24)$$

Equation (5-22) now becomes

$$C_0 = ek R_{yn}(\tau) p(\tau) + \frac{(ek)^2}{2} \frac{d}{d\tau} [R_{nn}(\tau) p(\tau)] + \frac{(ek)^3}{6} \frac{d^2}{d\tau^2} [R_{yn}(\tau) p(\tau)] \quad (5-25)$$

Input Signal
 $n(t, \theta_1)$



Feedback Signal
 $y(t, \theta_2(t))$

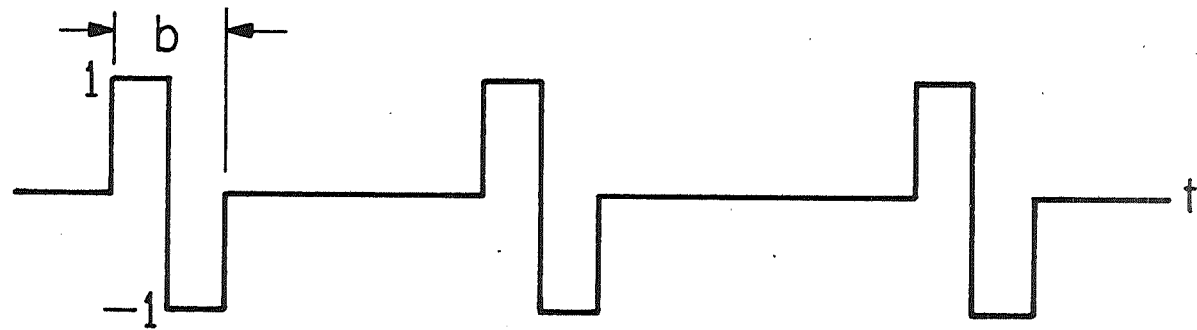


Figure 13.

Therefore, for the given input and feedback functions in Figure 13, Equation (5-25) could be solved as a second-order differential equation for the delay error density of an "Early Late Gate" tracking system. The solution would represent an approximate solution to the infinite series Smoluchowski equation. A computer solution similar to that used in Chapter 3 would be applicable to the solution of Equation (5-25).

REFERENCES

1. Viterbi, A.J., Principles of Coherent Communication, McGraw-Hill, Inc. (1966).
2. Davenport, Jr., W.B., and W.L. Root, Random Signals and Noise, McGraw-Hill, Inc. (1958).
3. Middleton, D., Introduction to Statistical Communication Theory, McGraw-Hill, Inc. (1960).
4. Papoulis, A., Probability, Random Variables, and Stochastic Processes, McGraw-Hill, Inc. (1965).
5. O'Niell, E. and Karp, S. and Gagliardi, R., "Communication Theory for the Free Space Optical Channel", Proc. of the IEEE, October 1970.
6. Karp, S., "A Statistical Model for Radiation with Applications to Optical Communications", Ph.D. Dissertation, University of Southern California (January 1967).
7. Anderson, L.K., and B.J. McMurty, "High Speed Photodetectors", Proceedings of the IEEE, Volume 54, Number 10 (October 1966).
8. Reiffen, B., and H. Sherman, "An Optimum Demodulator for Poisson Processes; Photo Source Detectors", Proceedings of the IEEE, (October 1963).
9. Bar-David, Israel, "Communication Under Poissonian Regime", Israel Ministry of Defense, Scientific Department, Report No. 40/07-526 (January 1968).
10. Parzen, E., Stochastic Processes, Holden Day, Inc. (1962).
11. Lindsey, William C., "Nonlinear Analysis and Synthesis of Generalized Tracking Systems", USCEE Technical Report 317, (December 1968).
12. Pratt, William K., Laser Communication Systems, John Wiley & Sons, Inc., (1969).
13. Coddington, Earl A., and Norman Levinson, Theory of Ordinary Differential Equations, McGraw-Hill Book Company, Inc. (1955).
14. Ince, E. L., Ordinary Differential Equations, Dover Publications, Inc., (1956).

15. Boyce, William E., and Richard C. DiPrima, Elementary Differential Equations and Boundary Value Problems, John Wiley and Sons, Inc., (1965).
16. Kolmogorov, A.N., "On Analytical Methods in Probability Theory", Math. Ann., Vol. 104, pp. 415-458 (in German), (1931).
17. Stratonovich, R.L., Topics in the Theory of Random Noise, Vol. 1, New York: Gordon and Breach, (1963).

USG
Engineering

